
LaVCa: LLM-assisted Visual Cortex Captioning

Takuya Matsuyama^{1,2} Shinji Nishimoto^{† 1,2} Yu Takagi^{† 1,2,3}

Abstract

Understanding the property of neural populations (or voxels) in the human brain can advance our comprehension of human perceptual and cognitive processing capabilities and contribute to developing brain-inspired computer models. Recent encoding models using deep neural networks (DNNs) have successfully predicted voxel-wise activity. However, interpreting the properties that explain voxel responses remains challenging because of the black-box nature of DNNs. As a solution, we propose LLM-assisted Visual Cortex Captioning (LaVCa), a data-driven approach that uses large language models (LLMs) to generate natural-language captions for images to which voxels are selective. By applying LaVCa for image-evoked brain activity, we demonstrate that LaVCa generates captions that describe voxel selectivity more accurately than the previously proposed method. Furthermore, the captions generated by LaVCa quantitatively capture more detailed properties than the existing method at both the inter-voxel and intra-voxel levels. Furthermore, a more detailed analysis of the voxel-specific properties generated by LaVCa reveals fine-grained functional differentiation within regions of interest (ROIs) in the visual cortex and voxels that simultaneously represent multiple distinct concepts. These findings offer profound insights into human visual representations by assigning detailed captions throughout the visual cortex while highlighting the potential of LLM-based methods in understanding brain representations. Please check out our webpage at <https://sites.google.com/view/lavca-llm/>.

1. Introduction

A primary goal of computer vision is to build systems capable of processing and understanding the complex visual world in a manner akin to human perception. Studying how the human brain—with its advanced visual functions—forms its visual representations deepens our understanding of the brain’s visual network and holds promise for developing next-generation computer vision models.

To understand how the human brain represents visual stimuli from the external world, researchers have used encoding models that predict voxel-level (the spatial measurement unit of fMRI) brain activity measured during the presentation of images or videos (Naselaris et al., 2011). These models typically use features derived from theoretical or data-driven hypotheses to map from stimulus properties to voxel responses (Kay et al., 2008; Nishimoto et al., 2011; Naselaris et al., 2011; Huth et al., 2012). Many such models use simple, interpretable features—for instance, low-level visual features generated by filters rooted in theoretical models or high-level visual features representing words using one-hot encoding—to infer voxel properties through the correlation between feature-based predictions and actual brain responses.

However, because the human brain solves highly complex real-world tasks, relying solely on a small number of interpretable parameters may be insufficient (Kriegeskorte & Douglas, 2018). Recent advances in deep neural networks (DNNs), which effectively handle real-world tasks through a large number of parameters, have enabled more accurate predictions of brain activity by leveraging the complex representations extracted by DNNs (Güçlü & Van Gerven, 2015; Schrimpf et al., 2021; Takagi & Nishimoto, 2023; Denk et al., 2023; Antonello et al., 2024). Nevertheless, because of their black-box nature, interpreting how these DNN-based features map to individual voxels remains challenging (Abnar et al., 2019). Although group-level interpretations—representing many voxels in terms of a small set of universal, interpretable axes—are possible (Huth et al., 2016; Lescroart & Gallant, 2019; Nakagi et al., 2024), voxel-level interpretation is critical for exploring more nuanced aspects of brain representations.

In this study, we address the difficulty of voxel-level interpre-

[†]Equal last author ¹Osaka University, Japan ²National Institute of Information and Communications Technology, Japan ³National Institute of Informatics, Research and Development Center for Large Language Models, Japan. Correspondence to: Shinji Nishimoto <nishimoto.shinji.fbs@osaka-u.ac.jp>, Yu Takagi <yu-takagi@nii.ac.jp>.

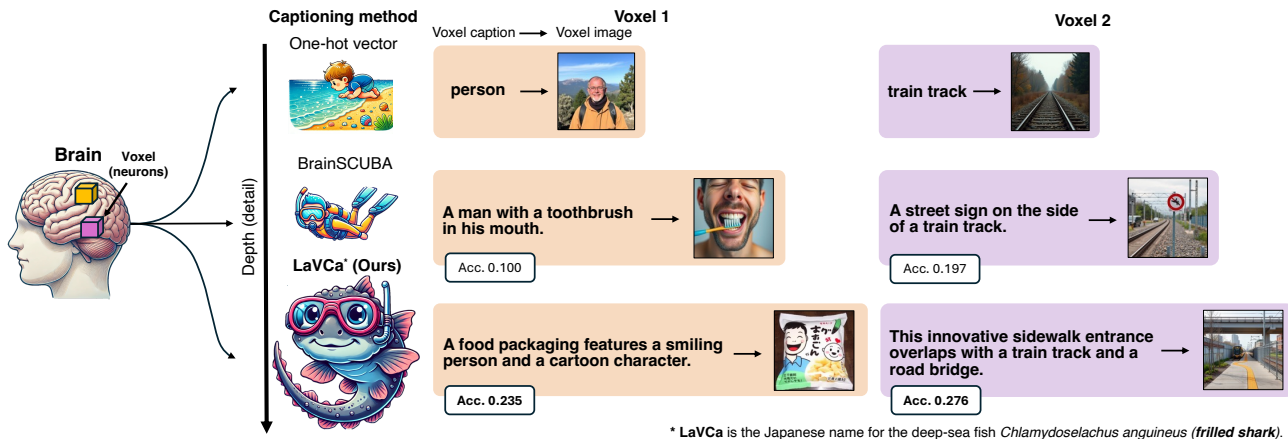


Figure 1. Illustration of our paper. Our proposed method, LaVCa, generates text captions that explain voxel selectivity and surpass existing approaches, such as one-hot vectors and BrainSCUBA, enabling a more detailed description of the properties of visual cortex voxels.

tation with a new method called LLM-assisted Visual Cortex Captioning (LaVCa), which generates data-driven captions for individual voxels (Figure 1). LaVCa proceeds in four steps: (1) building voxel-wise encoding models for brain activity evoked by images, (2) identifying the optimal images for each voxel’s encoding model using an augmented image dataset (3) generating captions for these optimal images, and (4) creating concise summaries from those captions. By leveraging large language models (LLMs) with access to a vast, open-ended vocabulary, LaVCa generates diverse inter-voxel captions. Moreover, generating captions from multiple keywords enables us to capture diverse intra-voxel properties. Our contributions are as follows:

1. We propose LLM-assisted Visual Cortex Captioning (LaVCa), a data-driven technique that leverages LLMs to generate natural language captions of voxel-level visual selectivity.
2. We demonstrate that LaVCa produces more accurate captions than the earlier method BrainSCUBA (Luo et al., 2023) and better characterizes voxel-wise visual selectivity through brain activity prediction.
3. We also demonstrate that LaVCa can generate highly interpretable and accurate captions without sacrificing information from the optimal images (Figure 2).
4. The captions generated by LaVCa quantitatively capture more detailed properties than the existing method at both the inter-voxel and intra-voxel levels.
5. More detailed analysis of the voxel-specific properties generated by LaVCa reveals fine-grained functional differentiation within regions of interest (ROIs) in the visual cortex and voxels that simultaneously represent multiple distinct concepts.

2. Related Work

Encoding models have been widely used in neuroscience to interpret neural representations (Kay et al., 2008; Nishimoto et al., 2011; Naselaris et al., 2011; Huth et al., 2012). These studies typically use interpretable low-level visual features and high-level semantic features, such as one-hot encodings,

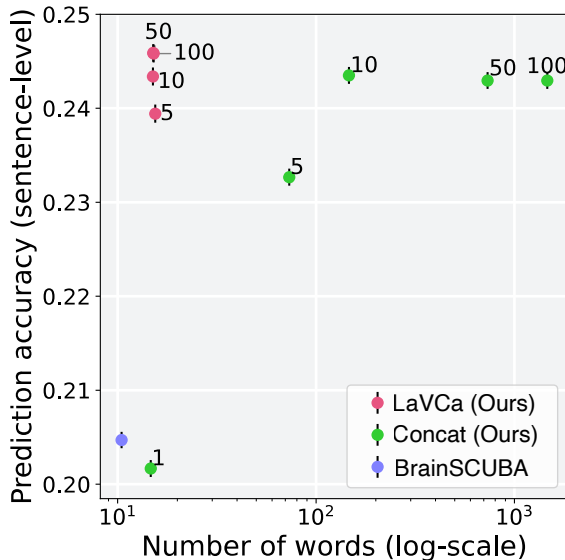


Figure 2. The relationship between sentence-level prediction performance and the number of words in voxel captions for a single subject (subj01). The number following “LaVCa” indicates the number of optimal images used for summarization, while the number following “Concat” indicates the number of concatenated captions from the optimal images. Error bars indicate the standard error. LaVCa explains the properties of voxels well using a small number of words.

permitting the interpretation of individual voxels.

Encoding models that rely on features extracted from DNNs can explain brain activity more effectively than those using simpler, more interpretable features (Güçlü & Van Gerven, 2015; Schrimpf et al., 2021; Takagi & Nishimoto, 2023; Antonello et al., 2024); however, their complexity complicates voxel-level interpretation. Consequently, several methods aggregate all voxels into a limited number of universal and interpretable axes (Huth et al., 2016; Lescroart & Gallant, 2019; Nakagi et al., 2024).

More recently, to enable finer analyses of neural representations at the voxel level, data-driven approaches have been proposed to generate natural-language descriptions of voxel selectivity (Luo et al., 2023; Singh et al., 2023). BrainSCUBA (Luo et al., 2023), for example, is an end-to-end method that uses an existing image captioning model to produce voxel-wise captions for the visual cortex. Similarly, SASC (Singh et al., 2023) uses an fMRI dataset recorded during speech listening (LeBel et al., 2023), uses an LLM to merge multiple short phrases—those with the highest predicted voxel activations—into a single, data-driven caption, thus describing the semantic properties of voxels.

Our proposed method also generates data-driven voxel captions but differs in several ways. First, BrainSCUBA is constrained to pre-existing, end-to-end image captioning models. In contrast, our approach divides the task into (i) identifying an optimal set of images and (ii) converting these images into a caption, allowing us to use any vision model aligned with language and any LLM with advanced language capabilities without requiring specialized fine-tuning. Furthermore, although SASC uses an LLM to create voxel captions, it primarily synthesizes short, low-information phrases (e.g., trigrams), producing only simple keyword-based captions. In contrast, our method summarizes more diverse and informative text and then uses these extracted keywords to compose a complete sentence, capturing a richer range of voxel-level properties.

3. Methods

3.1. fMRI dataset

This study uses the Natural Scenes Dataset (NSD) (Allen et al., 2022) following the same experimental conditions as in BrainSCUBA. The NSD consists of data collected over 30 to 40 sessions using a 7 Tesla fMRI scanner, with each participant viewing 10,000 images, repeated three times. We analyze data from the four participants (Subject 01, Subject 02, Subject 05, and Subject 07) who completed all imaging sessions. The images and captions used in NSD are drawn from MS COCO and resized to 224×224 pixels to align with the input requirements of the vision models used. We average the brain activity data for each subject across

repeated trials of the same image to improve the signal-to-noise ratio. Up to 9,000 images per subject are used as training data, and the remaining 1,000 images are reserved for testing. We use the preprocessed scans with a resolution of 1.8 mm provided by NSD for the functional data. We use single-trial beta weights estimated via a generalized linear model (GLM) within ROIs. Moreover, we standardize the response of each voxel to have a mean of zero and a variance of one within each session. We use the ROIs provided by NSD, which include early and higher-level (ventral) visual areas and face, place, body, and word-selective regions.

3.2. LLM-assisted Visual Cortex Captioning (LaVCa)

We propose a method, **LaVCa (LLM-assisted Visual Cortex Captioning)**, to automatically generate data-driven natural language captions that characterize each voxel’s selectivity in the visual cortex. LaVCa consists of four stages (Figure 3):

1. Construct voxel-wise encoding models for each subject while they view natural images.
2. Identify the optimal image set by finding the top- N images that most strongly activate each voxel (according to the trained encoding models).
3. Generate captions for these optimal images using a Multimodal LLM (MLLM) for summarization by an LLM in the next step.
4. Derive concise voxel captions by extracting and filtering keywords from the image captions, then feeding these keywords into a “Sentence Composer.”

3.2.1. ENCODING MODEL CONSTRUCTION

First, we construct voxel-wise encoding models to predict each voxel’s activity in response to natural images (Figure 3a). For ease of comparison with BrainSCUBA, we use the projection layer of CLIP’s vision branch (Radford et al., 2021), using the same pretrained checkpoint used in BrainSCUBA (A.2.2 for details on pretrained model checkpoints). Hereafter, we refer to CLIP’s vision branch as “CLIP-Vision”. Because the code for BrainSCUBA is not publicly available, we implement it in-house. Both the dataset used for the softmax projection and the training approach for the encoding model differ from those in the original paper (A.2.3 for details). We estimate the encoding model weights using L2-regularized linear regression on the NSD training set.

3.2.2. EXPLORATION OF OPTIMAL IMAGE SETS FOR VOXELS

Next, we identify the optimal image set for each voxel (Figure 3b). We compute the inner product between the voxel’s

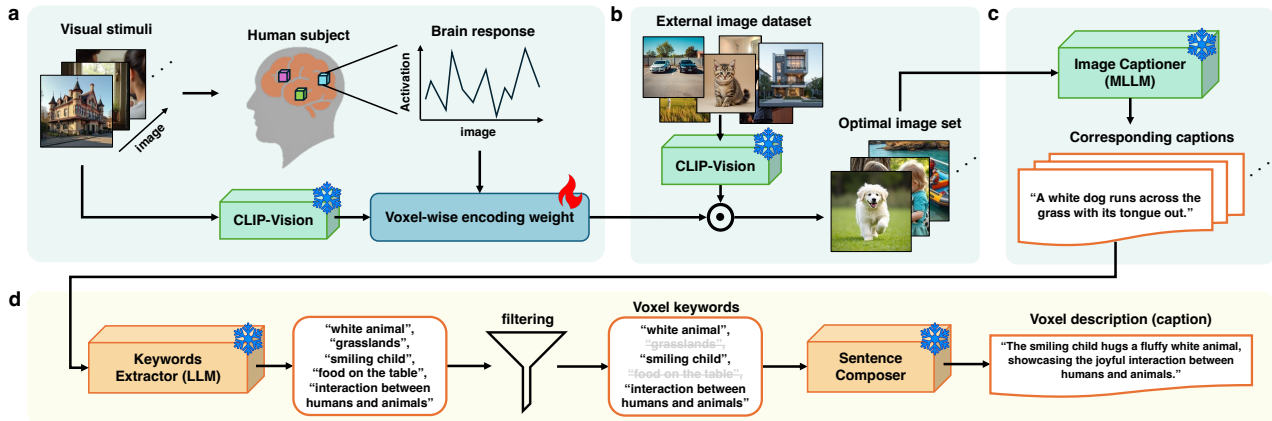


Figure 3. Architecture of LaVCA. (a) We construct a voxel-wise encoding model for a human subject’s brain activity data (measured using fMRI) while viewing images, using CLIP-Vision latent representations. The encoding weight is obtained through ridge regression. (b) We identify the optimal images for a given voxel by calculating the inner product between the CLIP-Vision latent representations of external image datasets and the voxel’s trained encoding weight, selecting the top- N images (the “optimal image set”) that produce the highest predicted activation. (c) Next, we use a Multimodal LLM (MLLM) to generate captions for each optimal image set, allowing an LLM to interpret them. (d) Finally, we prompt an LLM to extract keywords from the captions, filter these keywords, and feed them into a “Sentence Composer,” producing a concise voxel caption.

encoding weight and CLIP-Vision latent representations from a large-scale external dataset (distinct from NSD) to obtain predicted voxel responses for each image. We then select the top- N images that generate the highest predicted activation. This process is equivalent to calculating the predicted responses of each voxel for every image. This study uses approximately 1.7 million images from OpenImages-v6 (Kuznetsova et al., 2020) (the same dataset used in our in-house BrainSCUBA).

3.2.3. CAPTIONING OPTIMAL IMAGE SETS WITH MLLM

To enable an LLM to interpret each voxel’s optimal image set, we first generate captions for these image sets using an MLLM. We use MiniCPM-V (Yao et al., 2024) with the prompt “Describe the image briefly.” For our accuracy evaluation, we also form a simple baseline by concatenating the top- N captions from the optimal image set.

3.2.4. GENERATING VOXEL CAPTIONS

Finally, we generate interpretable voxel captions from the image captions. First, we use an LLM to extract common keywords across the captions within each voxel’s optimal image set (Figure 3d). Following the in-context learning prompt approach from (Dunlap et al., 2024), we extract multiple keywords from the caption sets using an LLM (A2 for the prompt). We use *gpt-4o* (gpt-4o-2024-08-06 in the OpenAI API) as the LLM. In A.3, we investigate the effects of several hyperparameters on accuracy, including the number

of images in the optimal image sets, the number of extracted keywords, and the type of keywords extractor. To remove irrelevant or noisy keywords, we compute the cosine similarity between each keyword’s embedding from CLIP’s text branch (prompted as “A photo of {keyword}.”) and the encoding weight for that voxel, then apply a softmax threshold to retain only sufficiently relevant keywords. Hereafter, we refer to CLIP’s text branch as “CLIP-Text”. Next, we transform these filtered keywords into a sentence-level caption using the “Sentence Composer” from MeaCap (Zeng et al., 2024), initially designed to generate image captions from keyword sets. MeaCap can generate a caption by inputting the target image’s keywords into the Sentence Composer while referencing similarities to the image features. In this study, we replace image features with encoding weights so that the model composes a coherent sentence from the voxel-specific keywords (for details, see Section A.2.1).

3.3. Caption Evaluation

3.3.1. BRAIN ACTIVITY PREDICTION AT SENTENCE LEVEL

We predict brain activity based on sentence similarity to assess how accurately voxel captions describe voxel selectivity (Figure A3a). We hypothesize that a voxel caption capturing the true selectivity of a voxel should be more similar to the corresponding caption of an NSD image that strongly activates that voxel and less similar otherwise. Following (Singh et al., 2023), we:

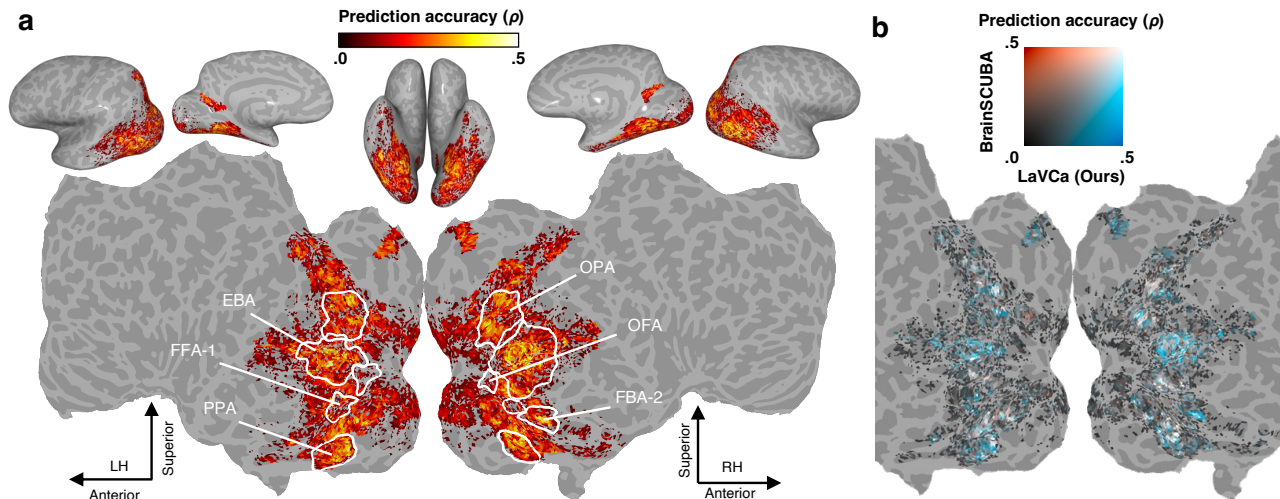


Figure 4. Mapping of brain activity prediction accuracy (subj01). (a) The sentence-level prediction performance is projected onto inflated cortical surfaces (top: lateral, medial, and dorsal views) and flattened cortical surfaces (bottom, with the occipital areas at the center) for both hemispheres. Voxels with significant prediction performance are color-coded (all colored voxels $P < 0.05$, FDR corrected). The white outlines indicate the ROIs that are among the top two in terms of the total voxel count across subjects for each semantic category—Body (Extra Striate Body Area; EBA, and Fusiform Body Area; FBA-2), Face (Fusiform Face Area; FFA-1, and Occipital Face Area; OFA), and Places (Parahippocampal Place Area; PPA, and Occipital Place Area; OPA). Word areas are shown in Figure A4. (b) A comparison of sentence-level prediction performance between our method, LaVCa, and the existing method, BrainSCUBA on the flattened cortical surface. If only one model exhibits significant prediction performance for a given voxel, the other model’s performance for that voxel is set to zero and color-coded accordingly.

1. Use a pretrained Sentence-BERT to compute text embeddings for each voxel caption and each NSD image caption.
2. Compute the cosine similarity between the voxel caption embedding and each NSD image caption embedding.
3. Treat this similarity value as the predicted activity for that voxel on that image.

We then calculate Spearman’s rank correlation coefficient (ρ) between these predicted values (sentence similarities) and the actual voxel activities. Statistical significance (one-tailed) is determined by comparing the observed correlation to a null distribution of correlations from two independent Gaussian random vectors of the same length, using a threshold of $P < 0.05$, followed by False Discovery Rate (FDR) correction.

3.3.2. BRAIN ACTIVITY PREDICTION AT IMAGE LEVEL

Because sentence-based evaluation can be influenced by non-visual linguistic features (e.g., sentence length), we also assess voxel selectivity using *image* similarity (Figure A3b). We use FLUX.1-schnell to create a *voxel image* and then compute vision embeddings (via CLIP-Vision) for both the generated voxel image and each NSD trial image. We

obtain an image-level metric of predicted brain activity by comparing these embeddings, focusing purely on visual content.

4. Results

4.1. Voxel Activity Prediction

To determine whether the generated captions accurately describe the properties of the voxels, we evaluate brain activity prediction at both the sentence and image levels. First, we map sentence-level prediction performance across inflated and flattened cortical surfaces (Figure 4a). These maps illustrate that LaVCa captions significantly predict voxel activity throughout the visual cortex ($P < 0.05$, FDR corrected). See Figure A4 for the results of all subjects.

Next, we compare LaVCa, the existing method BrainSCUBA, and a shuffled variant (LaVCa captions shuffled across voxels) at both the sentence and image levels, focusing on the top 5,000 voxels with the highest accuracy on the training data (Table 1). Our proposed method, LaVCa, outperforms BrainSCUBA ($P < 0.05$, paired t-test). This finding indicates that generating captions based on multiple keywords extracted from an optimal set of images provides a more accurate explanation of voxel selectivity. Furthermore, the marked drop in accuracy for the shuffled condition compared with the original LaVCa confirms that our evaluation

Table 1. Comparison of brain activity prediction accuracy at the sentence and image levels. For each subject, the mean and standard deviation of accuracy on the test data are displayed for the top 5,000 voxels with the highest accuracy on the train data.

Model	Sentence				Image			
	subj01	subj02	subj05	subj07	subj01	subj02	subj05	subj07
Shuffled	0.007 ± 0.199	0.058 ± 0.223	0.068 ± 0.243	0.009 ± 0.175	0.017 ± 0.163	0.052 ± 0.185	0.066 ± 0.204	0.009 ± 0.149
BrainSCUBA	0.207 ± 0.062	0.251 ± 0.071	0.264 ± 0.084	0.182 ± 0.065	0.188 ± 0.067	0.226 ± 0.070	0.250 ± 0.078	0.169 ± 0.069
LaVCa (Ours)	0.246 ± 0.066	0.287 ± 0.075	0.306 ± 0.084	0.218 ± 0.073	0.213 ± 0.072	0.250 ± 0.070	0.273 ± 0.079	0.187 ± 0.073

metric efficiently gauges whether captions describe voxel selectivity. Results for the top 1,000, 3,000, and 10,000 voxels appear in Table A2 and A3. After visualizing sentence-level prediction accuracy across the cortex, we find that LaVCa exceeds BrainSCUBA’s performance throughout the visual cortex (Figure 4b). See Figure A5 for the results of all subjects.

Finally, we examine whether LaVCa can generate concise and interpretable voxel captions without losing critical information in each voxel’s optimal image set. We compare two approaches from the perspective of interpretability by varying the number of optimal images used by LaVCa (Top- N) and by simply concatenating the captions of the optimal images (Concat- N). Figure 2 plots prediction accuracy against the average caption length on the horizontal axis, highlighting the trade-off between accuracy and interpretability. Concat- N achieves better accuracy as N increases (up to $N = 10$) but at the cost of a much longer caption, which can reduce interpretability. In contrast, LaVCa merges information across the optimal image set into a concise summary, retaining interpretability even as N grows and reaching accuracy comparable to Concat- N . Results for all participants are provided in Figure A6.

4.2. Lexical and Semantic Diversity Analysis

We next assess how effectively LaVCa captions capture both lexical and semantic diversity across voxels, focusing first on *inter-voxel* diversity (Table A4, left). For this quantitative evaluation, we use three metrics: (1) the total vocabulary size (excluding stop-words) across all voxel captions (Lexical); (2) the average variance across each dimension of the CLIP-Text embedding computed on all voxel captions (Semantic); and (3) the number of principal components (PCs) required to capture 90% of the variance of CLIP-Text embedding across captions in a principal component analysis (PCA; Semantic).

First, we evaluate the diversity of LaVCa captions compared with the existing method, BrainSCUBA. When averaged across subjects, LaVCa markedly outperforms BrainSCUBA in both lexical (16,922 vs. 3,193 in vocab. size) and semantic (0.0642 vs. 0.0588 in variance of embeddings; 219 vs. 127 in PCs required for 90% variance explained) diversity. These findings confirm that our open-ended LLM-based approach can produce richer word usage

and more meaningful captions across inter-voxel comparisons.

We evaluate the diversity of LaVCa captions compared with more detailed captions. BrainSCUBA leverages ClipCap (Mokady et al., 2021), a model that produces relatively simple image captions. We use the top-1 captions generated by the MLLM on the optimal image sets (equivalent to the case where $N = 1$ in Concat- N) to compare the diversity of LaVCa with more detailed captions. When averaged across subjects, Top-1 (13,959 vocab. size, 0.0638 avg. variance, 210 PCs) exhibits both a vocabulary range and semantic diversity close to LaVCa. However, LaVCa achieves a higher prediction accuracy (0.264 vs. 0.224), indicating that LaVCa can preserve robust brain activity prediction performance while enhancing the diversity of generated captions.

Next, we evaluate diversity from an *intra-voxel* perspective by comparing captions generated by three models in both lexical and semantic dimensions (Table A4, right). We use three metrics: (1) the vocabulary size of each voxel’s caption (Lexical), (2) the average sentence length in each voxel’s caption (Lexical), and (3) the average variance across all dimensions of Word2Vec embeddings of each caption’s words (excluding stop-words) (Semantic). When averaged across subjects, LaVCa markedly outperforms BrainSCUBA in both lexical (11.4 vs. 6.09 in vocab. size) and semantic (11.9 vs. 6.19 in avg. length; 0.0199 vs. 0.0160 in variance of semantic embeddings) diversity. This improvement suggests that LaVCa more precisely captures the fine-grained intra-voxel characteristics.

For examples of voxel captions and images from various OFA and PPA voxels—along with their corresponding quantitative metrics—compared across three models (LaVCa, BrainSCUBA, Top-1), see Figures A8, A9, A10, and A11.

4.3. ROI-level Diversity Analysis

Our results thus far illustrate that LaVCa generates more accurate voxel captions than BrainSCUBA and better reflects inter- and intra-voxel diversity. We now assess how LaVCa captions capture diversity within known ROI, such as the OFA and PPA. These areas are conventionally associated with specific concepts (e.g., faces or places), (Gauthier et al., 2000; Haxby et al., 2000; Epstein & Kanwisher, 1998) yet

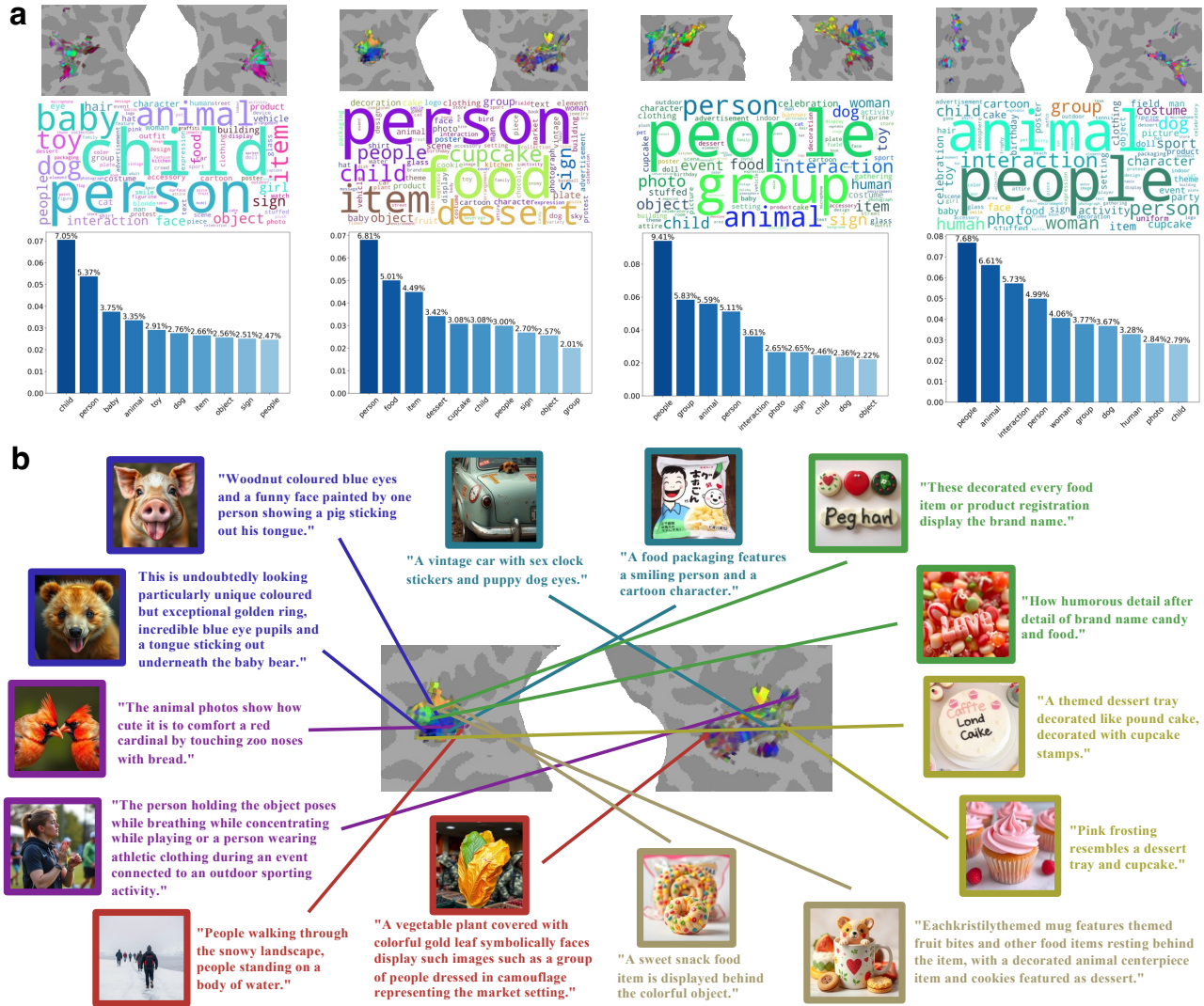


Figure 5. Interpretation of LaVCa captions in OFA. (a) The UMAP projection of caption text for all participants, visualized on a flatmap (top). A word cloud of the 100 most frequent words in these captions (middle), colored according to their location in the UMAP space. A bar graph of the top 10 most frequent words (bottom). (b) Visualization of the top two captions (by accuracy) for eight clusters on the flatmap (subj02). The images generated for each caption appear to the left or above the text. Voxels are connected to their corresponding captions and images by lines. The color of each caption and image border reflects the average UMAP color of all voxels in the cluster.

the extent of diversity within these ROIs remains unclear. We conduct a quantitative evaluation using LaVCa’s captions and generated images to analyze diversity that exists beyond the known selectivity in the ROI (Figures 5 and A7).

Quantitative Assessment. We determine how many distinct captions appear in each ROI by comparing the sentence-level prediction accuracy of each ROI when captions are maintained in their original form versus shuffled within the ROI (Figure 2). For each category (body, face, place, and word area), we select two ROIs with the largest total voxel count across all subjects, resulting in eight ROIs in total. In

all ROIs, shuffling reduces prediction accuracy significantly. For example, in the OFA, accuracy drops from 0.0945 (Original) to 0.0280 (Shuffled), a 3.3-fold decrease; in the PPA, accuracy falls from 0.213 (Original) to 0.151 (Shuffled), a 1.4-fold decrease. Thus, even in regions traditionally linked to particular concepts, voxels exhibit a range of distinct selectivities.

Qualitative Assessment. We next explore the semantic diversity of LaVCa captions in the OFA by applying UMAP to their CLIP-Text embeddings and visualizing the resulting distributions on a flatmap (Figure 5a, top). Each subject’s

Table 2. Average prediction accuracy with standard error across subjects when captions within each ROI are shuffled (Shuffled) versus used as is (Original).

	Body areas		Face areas		Place areas		Word areas	
	EBA	FBA-2	OFA	FFA-1	OPA	PPA	OWFA	VWFA-1
Shuffled	0.018±0.008	0.018±0.005	0.028±0.004	0.016±0.003	0.116±0.024	0.151±0.028	0.025±0.005	0.034±0.009
Original	0.157±0.005	0.125±0.010	0.095±0.009	0.111±0.003	0.200±0.022	0.213±0.027	0.084±0.013	0.158±0.007

OFA illustrates a broad spectrum of UMAP colors, indicating multiple meaningful clusters within an ROI known for face-selective responses. See Figure A7 for the results of the PPA.

To examine the word-level patterns within ROIs, we construct a word cloud from the top 100 most frequent words and a histogram of the top 10 words (Figure 5a, middle and bottom). We align the word cloud with the flatmap colors by obtaining the CLIP-Text embeddings for each word using the prompt “A photo of word.” We then apply the UMAP learned from the CLIP-Text embeddings of the captions to convert the top 100 words into the same UMAP space. While high-frequency words like “child,” “people,” and “animal” align with face or person-related content, the presence of terms such as “food” or “sign” suggests more diverse encoding.

Finally, to highlight how each caption and its corresponding voxel image relate to specific colors in semantic space, we project them onto a flatmap (Figure 5b). We divide the samples into eight clusters by labeling each of the three UMAP dimensions as “High” ($\geq 2/3$) or “Low” ($\leq 1/3$). From each cluster, we pick the two voxels with the highest prediction accuracy (or one if only one qualifies, or none if none qualify) and illustrate their captions and generated images.

In OFA, some captions are related to faces (e.g., “face,” “person,” “animal”), while particular voxels encoded more fine-grained features such as “eye,” “tongue,” or “smiling,” and other voxels encoded information like “animal,” “bear,” or “cardinal.” Thus, even within this ROI, there appears to be substantial functional differentiation among inter-voxel that extends beyond a generic “face” category. Moreover, we observe *intra-voxel* diversity, where a single caption incorporates multiple ideas (e.g., “A food packaging features a smiling person and a cartoon character”), suggesting that individual voxels can simultaneously encode several distinct concepts. These findings highlight the fine-grained functional specialization across inter-voxel within the ROI and the diverse nature of intra-voxel encoding beyond singular concepts. The results for all participants, visualizing the top two captions for each cluster directly in the UMAP space, can be found in Figures A12, A13, A14, and A15.

5. Discussion & Conclusions

In this study, we introduce a novel method called LaVCa, which leverages LLMs to produce data-driven, natural-language descriptions of voxel selectivity in the human visual cortex. The voxel captions generated by LaVCa exhibit higher accuracy and greater semantic diversity than those generated by the existing approach, BrainSCUBA. We attribute this improvement to our mechanism for integrating multiple keywords extracted by advanced LLMs, which enables a more comprehensive capture of the diverse selectivity patterns across voxels.

Despite the overall improvement in brain activity prediction, we observe that face-selective regions do not achieve accuracy levels as high as those in other ROIs (Figure 2). One reason may be that our current approach uses a Multimodal LLM (MLLM) to produce relatively simple captions for optimal images, often omitting important local features (e.g., “eyes,” “nose”) and focusing on more global terms (e.g., “face,” “person”). Consequently, the subsequent summarization step lacks access to these local details. Because our method relies on language descriptions, it has inherent limitations in capturing the fine-grained, local selectivity of these voxels. Incorporating recent techniques that visually interpret local voxel selectivity (Luo et al., 2024) could help address this gap.

Furthermore, while our current study describes voxel selectivity primarily in response to visual stimuli in the occipital cortex, there exist “multimodal voxels” in the brain that are simultaneously activated by auditory and linguistic information, and higher-order cognitive processes such as calculations, memory retrieval, and reasoning (Nakai & Nishimoto, 2020; 2022). Designing stimuli and experimental tasks encompassing diverse sensory inputs (e.g., auditory, textual) and cognitive challenges (e.g., recalling past events, performing reasoning tasks) is essential when interpreting such voxels. Because our approach uses LLM-based textual summarization, it can be adapted to represent a wide range of stimuli and cognitive states in text form, providing a unified framework for multimodal integration. Looking ahead, by jointly modeling images, semantic information, auditory features, and cognitive tasks, we anticipate capturing the brain’s integrated representation of both sensory and higher-order cognitive functions with greater accuracy.

Impact Statement

We introduce a data-driven method that uses a large language model to generate natural-language captions of voxel-level visual selectivity. Using the method detailed in this paper, we aim to provide a more fine-grained understanding of human visual function than previously achieved. We acknowledge that this human brain research could raise concerns regarding individual privacy. Although the present study examined relatively coarse-grained voxel-level data, we cannot dismiss the possibility that future advances in measurement and analysis techniques may enable the extraction of more detailed individual-specific information. In any case, obtaining explicit informed consent from participants remains crucial when collecting and using human brain activity data, as with the NSD dataset used in this study.

Acknowledgement

Y.T. was supported by PRESTO Grant Number JP-MJPR2316. S.N. was supported by KAKENHI JP24H00619 and JST JPMJCR24U2.

Author Contribution

Y.T. and S.N. proposed the research direction and advised the project. T.M. conceived the method and conducted all analyses. T.M. wrote the original draft, and all authors contributed to the manuscript writing.

References

- Abnar, S., Beinborn, L., Choenni, R., and Zuidema, W. Blackbox meets blackbox: Representational similarity and stability analysis of neural language models and brains. *arXiv preprint arXiv:1906.01539*, 2019.
- Allen, E. J., St-Yves, G., Wu, Y., Breedlove, J. L., Prince, J. S., Dowdle, L. T., Nau, M., Caron, B., Pestilli, F., Charest, I., et al. A massive 7t fmri dataset to bridge cognitive neuroscience and artificial intelligence. *Nature neuroscience*, 25(1):116–126, 2022.
- Antonello, R., Vaidya, A., and Huth, A. Scaling laws for language encoding models in fmri. *Advances in Neural Information Processing Systems*, 36, 2024.
- Bai, N., Iyer, R. A., Oikarinen, T., and Weng, T.-W. Describe-and-dissect: Interpreting neurons in vision networks with language models. *arXiv preprint arXiv:2403.13771*, 2024.
- Bau, D., Zhou, B., Khosla, A., Oliva, A., and Torralba, A. Network dissection: Quantifying interpretability of deep visual representations. In *Proceedings of the IEEE conference on computer vision and pattern recognition*, pp. 6541–6549, 2017.
- Bykov, K., Kopf, L., Nakajima, S., Kloft, M., and Höhne, M. Labeling neural representations with inverse recognition. *Advances in Neural Information Processing Systems*, 36, 2024.
- Denk, T. I., Takagi, Y., Matsuyama, T., Agostinelli, A., Nakai, T., Frank, C., and Nishimoto, S. Brain2music: Reconstructing music from human brain activity. *arXiv preprint arXiv:2307.11078*, 2023.
- Dunlap, L., Zhang, Y., Wang, X., Zhong, R., Darrell, T., Steinhardt, J., Gonzalez, J. E., and Yeung-Levy, S. Describing differences in image sets with natural language. In *Proceedings of the IEEE/CVF Conference on Computer Vision and Pattern Recognition*, pp. 24199–24208, 2024.
- Epstein, R. and Kanwisher, N. A cortical representation of the local visual environment. *Nature*, 392(6676):598–601, 1998.
- Gauthier, I., Tarr, M. J., Moylan, J., Skudlarski, P., Gore, J. C., and Anderson, A. W. The fusiform “face area” is part of a network that processes faces at the individual level. *Journal of cognitive neuroscience*, 12(3):495–504, 2000.
- Güçlü, U. and Van Gerven, M. A. Deep neural networks reveal a gradient in the complexity of neural representations across the ventral stream. *Journal of Neuroscience*, 35(27):10005–10014, 2015.
- Haxby, J. V., Hoffman, E. A., and Gobbini, M. I. The distributed human neural system for face perception. *Trends in cognitive sciences*, 4(6):223–233, 2000.
- He, X. Parallel refinements for lexically constrained text generation with bart. *arXiv preprint arXiv:2109.12487*, 2021.
- Hernandez, E., Schwettmann, S., Bau, D., Bagashvili, T., Torralba, A., and Andreas, J. Natural language descriptions of deep visual features. In *International Conference on Learning Representations*, 2021.
- Hoang-Xuan, N., Vu, M., and Thai, M. T. Llm-assisted concept discovery: Automatically identifying and explaining neuron functions. *arXiv preprint arXiv:2406.08572*, 2024.
- Huth, A. G., Nishimoto, S., Vu, A. T., and Gallant, J. L. A continuous semantic space describes the representation of thousands of object and action categories across the human brain. *Neuron*, 76(6):1210–1224, 2012.

- Huth, A. G., De Heer, W. A., Griffiths, T. L., Theunissen, F. E., and Gallant, J. L. Natural speech reveals the semantic maps that tile human cerebral cortex. *Nature*, 532(7600):453–458, 2016.
- Kalibhat, N., Bhardwaj, S., Bruss, C. B., Firooz, H., Sanjabi, M., and Feizi, S. Identifying interpretable subspaces in image representations. In *International Conference on Machine Learning*, pp. 15623–15638. PMLR, 2023.
- Kay, K. N., Naselaris, T., Prenger, R. J., and Gallant, J. L. Identifying natural images from human brain activity. *Nature*, 452(7185):352–355, 2008.
- Kriegeskorte, N. and Douglas, P. K. Cognitive computational neuroscience. *Nature neuroscience*, 21(9):1148–1160, 2018.
- Kuznetsova, A., Rom, H., Alldrin, N., Uijlings, J., Krasin, I., Pont-Tuset, J., Kamali, S., Popov, S., Mallocci, M., Kolesnikov, A., Duerig, T., and Ferrari, V. The open images dataset v4: Unified image classification, object detection, and visual relationship detection at scale. *IJCV*, 2020.
- La Tour, T. D., Eickenberg, M., Nunez-Elizalde, A. O., and Gallant, J. L. Feature-space selection with banded ridge regression. *NeuroImage*, 264:119728, 2022.
- LeBel, A., Wagner, L., Jain, S., Adhikari-Desai, A., Gupta, B., Morgenthal, A., Tang, J., Xu, L., and Huth, A. G. A natural language fmri dataset for voxelwise encoding models. *Scientific Data*, 10(1):555, 2023.
- Lescroart, M. D. and Gallant, J. L. Human scene-selective areas represent 3d configurations of surfaces. *Neuron*, 101(1):178–192, 2019.
- Li, Z., Chai, Y., Zhuo, T. Y., Qu, L., Haffari, G., Li, F., Ji, D., and Tran, Q. H. Factual: A benchmark for faithful and consistent textual scene graph parsing. *arXiv preprint arXiv:2305.17497*, 2023.
- Luo, A. F., Henderson, M. M., Tarr, M. J., and Wehbe, L. Brainscuba: Fine-grained natural language captions of visual cortex selectivity. *arXiv preprint arXiv:2310.04420*, 2023.
- Luo, A. F., Yeung, J., Zawar, R., Dewan, S., Henderson, M. M., Wehbe, L., and Tarr, M. J. Brain mapping with dense features: Grounding cortical semantic selectivity in natural images with vision transformers. *arXiv preprint arXiv:2410.05266*, 2024.
- Mokady, R., Hertz, A., and Bermano, A. H. Clip-cap: Clip prefix for image captioning. *arXiv preprint arXiv:2111.09734*, 2021.
- Mu, J. and Andreas, J. Compositional explanations of neurons. *Advances in Neural Information Processing Systems*, 33:17153–17163, 2020.
- Nakagi, Y., Matsuyama, T., Koide-Majima, N., Yamaguchi, H. Q., Kubo, R., Nishimoto, S., and Takagi, Y. Unveiling multi-level and multi-modal semantic representations in the human brain using large language models. *bioRxiv*, pp. 2024–02, 2024.
- Nakai, T. and Nishimoto, S. Quantitative models reveal the organization of diverse cognitive functions in the brain. *Nature communications*, 11(1):1142, 2020.
- Nakai, T. and Nishimoto, S. Representations and decodability of diverse cognitive functions are preserved across the human cortex, cerebellum, and subcortex. *Communications Biology*, 5(1):1245, 2022.
- Naselaris, T., Kay, K. N., Nishimoto, S., and Gallant, J. L. Encoding and decoding in fmri. *Neuroimage*, 56(2):400–410, 2011.
- Nishimoto, S., Vu, A. T., Naselaris, T., Benjamini, Y., Yu, B., and Gallant, J. L. Reconstructing visual experiences from brain activity evoked by natural movies. *Current biology*, 21(19):1641–1646, 2011.
- Oikarinen, T. and Weng, T.-W. Clip-dissect: Automatic description of neuron representations in deep vision networks. *arXiv preprint arXiv:2204.10965*, 2022.
- Radford, A., Kim, J. W., Hallacy, C., Ramesh, A., Goh, G., Agarwal, S., Sastry, G., Askell, A., Mishkin, P., Clark, J., et al. Learning transferable visual models from natural language supervision. In *International conference on machine learning*, pp. 8748–8763. PMLR, 2021.
- Schrimpf, M., Blank, I. A., Tuckute, G., Kauf, C., Hosseini, E. A., Kanwisher, N., Tenenbaum, J. B., and Fedorenko, E. The neural architecture of language: Integrative modeling converges on predictive processing. *Proceedings of the National Academy of Sciences*, 118(45):e2105646118, 2021.
- Schuhmann, C., Beaumont, R., Vencu, R., Gordon, C., Wightman, R., Cherti, M., Coombes, T., Katta, A., Mullis, C., Wortsman, M., et al. Laion-5b: An open large-scale dataset for training next generation image-text models. *Advances in Neural Information Processing Systems*, 35: 25278–25294, 2022.
- Singh, C., Hsu, A. R., Antonello, R., Jain, S., Huth, A. G., Yu, B., and Gao, J. Explaining black box text modules in natural language with language models, 2023. URL <https://arxiv.org/abs/2305.09863>.

- Takagi, Y. and Nishimoto, S. High-resolution image reconstruction with latent diffusion models from human brain activity. In *Proceedings of the IEEE/CVF Conference on Computer Vision and Pattern Recognition*, pp. 14453–14463, 2023.
- Wu, T.-Y., Lin, Y.-X., and Weng, T.-W. And: Audio network dissection for interpreting deep acoustic models. *arXiv preprint arXiv:2406.16990*, 2024.
- Yao, Y., Yu, T., Zhang, A., Wang, C., Cui, J., Zhu, H., Cai, T., Li, H., Zhao, W., He, Z., Chen, Q., Zhou, H., Zou, Z., Zhang, H., Hu, S., Zheng, Z., Zhou, J., Cai, J., Han, X., Zeng, G., Li, D., Liu, Z., and Sun, M. Minicpm-v: A gpt-4v level mllm on your phone. *arXiv preprint 2408.01800*, 2024.
- Zeng, Z., Xie, Y., Zhang, H., Chen, C., Chen, B., and Wang, Z. Meacap: Memory-augmented zero-shot image captioning. In *Proceedings of the IEEE/CVF Conference on Computer Vision and Pattern Recognition*, pp. 14100–14110, 2024.

A. Appendix

A.1. Full Related Work

A.1.1. INTERPRETING THE REPRESENTATIONS OF THE BRAIN’S NEURONS.

Encoding models have long been used in neuroscience to interpret neural representations within the brain (Kay et al., 2008; Nishimoto et al., 2011; Naselaris et al., 2011; Huth et al., 2012). These studies used interpretable features, such as low-level visual attributes, or high-level semantic features, such as one-hot encoding of words, for straightforward voxel-wise interpretation.

Recent approaches use features derived from DNNs and have demonstrated higher explanatory power for brain activity than those using simpler, more interpretable features (Güçlü & Van Gerven, 2015; Schrimpf et al., 2021; Takagi & Nishimoto, 2023; Antonello et al., 2024). However, the interpretability of these DNN-based encoding models remains challenging, leading to the development of methods that condense the entire set of voxels into a small number of universal and interpretable axes (Huth et al., 2016; Lescroart & Gallant, 2019; Nakagi et al., 2024).

Recent approaches propose data-driven methods to describe the properties of individual brain voxels using natural language (Luo et al., 2023; Singh et al., 2023) when analyzing brain representations at a finer, voxel-wise level. BrainSCUBA (Luo et al., 2023) is an end-to-end method that uses an existing image captioning model, which provides voxel-wise captions of the visual cortex in a data-driven manner. BrainSCUBA projects each voxel’s encoding weight onto the image feature space via dot-product attention, identifies regions of highest similarity, and then uses a text decoder to generate captions describing the images to which the voxel is most selective. This approach provides a data-driven natural-language description of voxel selectivity without additional training. Similarly, SASC (Singh et al., 2023) uses fMRI data collected during speech listening (LeBel et al., 2023) to identify the short phrases that most strongly activate each voxel. It then uses an LLM to combine these short phrases into a single, data-driven caption describing each voxel’s semantic properties.

Our proposed method also generates data-driven voxel captions but differs in several ways. First, BrainSCUBA is constrained to pre-existing, end-to-end image captioning models. In contrast, our approach divides the task into (i) identifying an optimal set of images and (ii) converting these images into a caption, allowing us to use any vision model aligned with language and any LLM with advanced language capabilities without requiring specialized fine-tuning. Furthermore, although SASC uses an LLM to create voxel captions, it primarily synthesizes short, low-information phrases (e.g., trigrams), producing only simple keyword-based captions. In contrast, our method summarizes more diverse and informative text and then uses these extracted keywords to compose a complete sentence, capturing a richer range of voxel-level properties.

A.1.2. INTERPRETING THE REPRESENTATIONS OF ARTIFICIAL NEURONS IN DNNs

Interpreting artificial neurons is a key challenge in understanding how DNNs process information. We can potentially examine human neural representations at a finer granularity by applying the data-driven and highly accurate interpretation methods developed for artificial neurons to analyze human brain voxels.

Numerous studies have aimed to associate artificial neurons with human-interpretable concepts (Bau et al., 2017; Mu & Andreas, 2020; Oikarinen & Weng, 2022; Kalibhat et al., 2023; Bykov et al., 2024). These methods link neurons to textual concepts by comparing neuron output feature maps with outputs from segmentation models. However, these approaches are constrained by predefined concept sets or limited to the dataset’s words and phrases. MILAN (Hernandez et al., 2021) introduced a generative approach, enabling adaptation to different domains and tasks, but it requires annotated data, which poses challenges for scalable applications.

LLMs permit open-ended descriptions of artificial neurons without additional model training (Singh et al., 2023; Bai et al., 2024; Wu et al., 2024; Hoang-Xuan et al., 2024). Analogous to these methods, our study also leverages LLMs to generate open-ended concepts for **brain** neurons rather than artificial neurons, seeking flexible and diverse interpretations that do not depend on predefined vocabularies.

A.2. Implementaion Details

A.2.1. GENERATING VOXEL CAPTIONS

In this study, we generate sentence-level captions from keywords by leveraging the “Sentence Composer” proposed in the image captioning model, MeaCap (Zeng et al., 2024)—referred to in the MeaCap paper as a “keywords-to-sentence LM.”

In MeaCap, a target image is first matched with similar candidate captions via CLIP-Text embeddings. Each candidate caption is parsed into Subject–Predicate–Object triplets using TextGraphParser (Li et al., 2023), which produces keywords. While TextGraphParser can be used in our approach to extract keywords from candidate captions, it treats each word in the caption individually, limiting its ability to capture higher-level concepts (e.g., “animal” as a hypernym of “dog” and “cat”) or to derive keywords that depend on sentence-level understanding (e.g., *interaction between humans and animals*). We overcome these limitations using LLMs (through in-context learning) as our keyword extraction model. We further verify the effectiveness of LLM-based keyword extraction by comparing it against the baseline that uses TextGraphParser (A.3).

After extracting keywords, MeaCap feeds the extracted keywords into CBART (He, 2021), a lexically constrained language model (Sentence Composer). CBART adopts an encoder–decoder structure, where the encoder predicts actions at the token level, such as copying (using the token as-is), substituting (replacing it with a new token), or inserting new tokens. The decoder then selects the token with the highest conditional probability when substitution or insertion is needed and iteratively refines the output until all tokens are predicted to be copies. In MeaCap (Zeng et al., 2024), the decoder’s choices are guided not only by conditional probabilities but also by the summed similarity of the generated caption’s CLIP-Text latent representation with (1) the target image’s CLIP-Vision latent representation and (2) the CLIP-Text latent representations of the top- N most similar external captions. This strategy enables inserting or substituting new words more relevant to the image. Our study replaces the image features used in MeaCap with the voxel-wise encoding weight, substituting and inserting new words based on the encoding weight. By doing so, we generate voxel captions from keywords while preserving the core mechanism of MeaCap’s Sentence Composer.

A.2.2. PRETRAINED CHECKPOINTS

Our experiments use the CLIP ViT-B/32 weights provided on GitHub¹ for encoding, caption generation, and image-level caption evaluation. For captioning each voxel’s optimal image set, we use MLLM model MiniCPM-Llama3-V2.5, available on Hugging Face². We extract keywords from the resulting optimal captions using *gpt-4o* (gpt-4o-2024-08-06) via the OpenAI API for the primary analysis and Llama3.1–70B from Hugging Face³ for the ablation study (A.3). For the sentence-level caption evaluation, we calculate sentence similarity using Sentence-BERT from Hugging Face⁴. Moreover, for image-level caption evaluation, we generate voxel images from voxel captions using an image generation model on Hugging Face⁵.

A.2.3. BRAINSCUBA

Because the BrainSCUBA codebase is not publicly available, we implemented it ourselves for this study. In BrainSCUBA, the encoding weights (linear layers) are learned using gradient descent. In our implementation, consistent with our proposed method, we trained the encoding weights using L2-regularized linear regression from the *himalaya* library package⁶ (La Tour et al., 2022).

Moreover, BrainSCUBA projects each voxel’s encoding weight into image space using a dataset of 2 million images, combining OpenImages (Kuznetsova et al., 2020) and LAION-A v2 (6+ subset) (Schuhmann et al., 2022). However, the specific images selected from each dataset are not disclosed. We ensure a fair and dataset-independent comparison by relying solely on the 1.7 million images from OpenImages (the same dataset used by our proposed method, LaVCa). We leverage the training set of the subset that is accompanied by bounding boxes, object segmentations, visual relationships, and localized narratives.

For other hyperparameters, we tested temperature values of 1.0, 1/10, 1/100, 1/150 (the value used in the BrainSCUBA paper), and 1/500 for the softmax projection (Figure A1). We used beam search with a beam width of 5 to generate the text decoder’s caption as described in the BrainSCUBA paper.

¹<https://github.com/openai/CLIP>

²<https://huggingface.co/openbmb/MiniCPM-Llama3-V-2.5>

³<https://huggingface.co/meta-llama/Llama-3.1-70B-Instruct>

⁴<https://huggingface.co/sentence-transformers/all-MiniLM-L6-v2>

⁵<https://huggingface.co/black-forest-labs/FLUX.1-schnell>

⁶<https://github.com/gallantlab/himalaya>

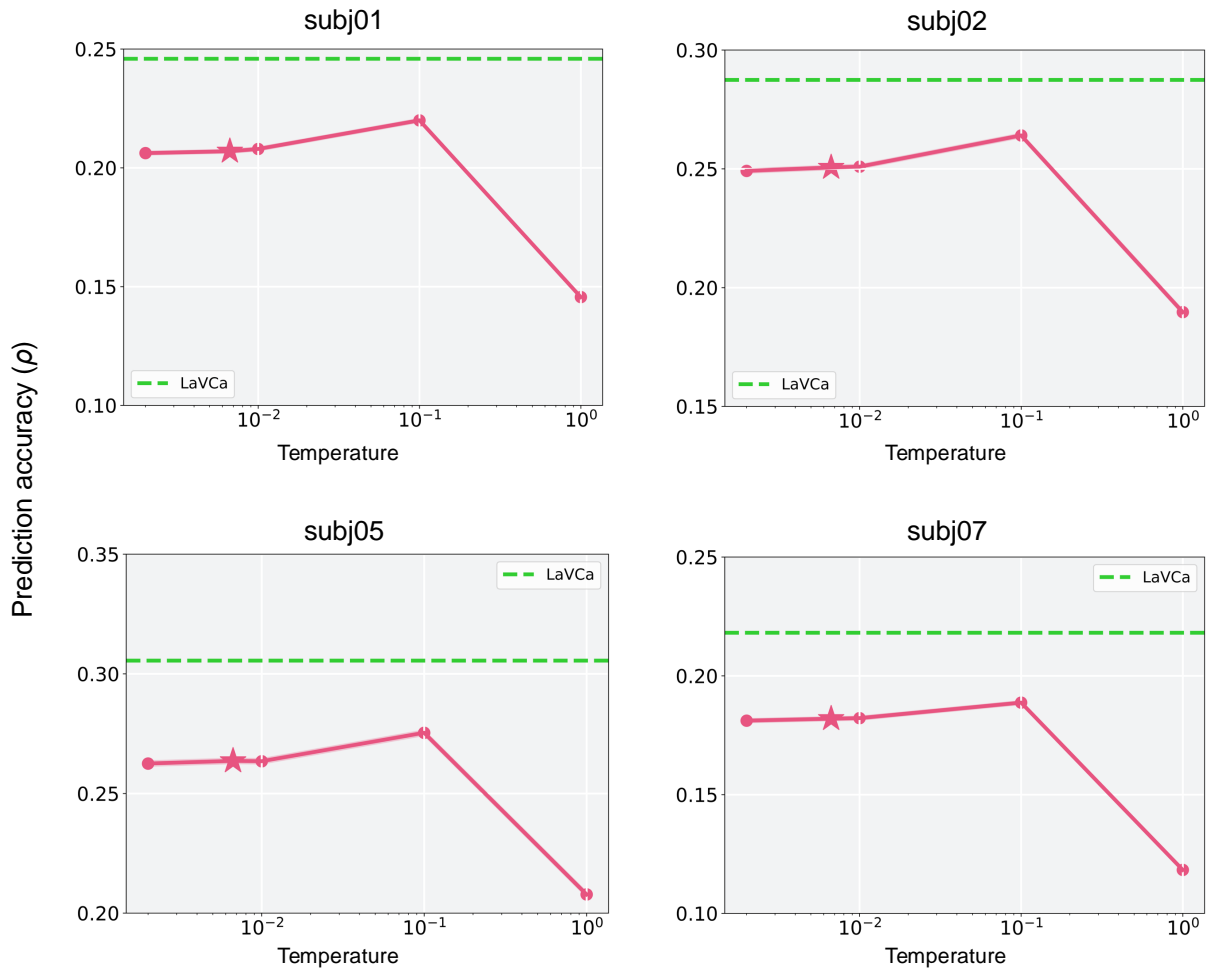


Figure A1. The change in accuracy of BrainSCUBA with respect to temperature. The error bars represent standard error. Moreover, the star markers on the plot indicate the point where the temperature is set to $1/150$, as adopted in the original BrainSCUBA paper. The green line represents the average value of LaVCa.

Table A1. Comparison of sentence-level brain activity prediction accuracy using different hyperparameters. The accuracy represents the mean and standard deviation of brain activity prediction accuracy for the top 5000 voxels in the test data at the text level. The top 5000 voxels were selected based on their prediction accuracy in the training data.

Parameter	Setting	subj01	subj02	subj05	subj07
Num. of images	5	0.2394 ± 0.0681	0.2786 ± 0.0730	0.2936 ± 0.0830	0.2092 ± 0.0730
	10	0.2434 ± 0.0678	0.2814 ± 0.0724	0.2966 ± 0.0826	0.2120 ± 0.0737
	50	0.2459 ± 0.0663	0.2874 ± 0.0748	0.3055 ± 0.0840	0.2182 ± 0.0730
	100	0.2458 ± 0.0672	0.2852 ± 0.0739	0.3011 ± 0.0834	0.2154 ± 0.0721
Num. of keywords	1	0.2374 ± 0.0660	0.2738 ± 0.0734	0.2949 ± 0.0849	0.2066 ± 0.0719
	5	0.2459 ± 0.0663	0.2874 ± 0.0748	0.3055 ± 0.0840	0.2182 ± 0.0730
	10	0.2410 ± 0.0671	0.2790 ± 0.0736	0.2956 ± 0.0842	0.2116 ± 0.0742
Extraction model	TextGraphParser	0.2416 ± 0.0667	0.2764 ± 0.0731	0.2955 ± 0.0841	0.2048 ± 0.0706
	Llama3.1-70B	0.2375 ± 0.0671	0.2812 ± 0.0749	0.2984 ± 0.0846	0.2140 ± 0.0734
	gpt-4o	0.2459 ± 0.0663	0.2874 ± 0.0748	0.3055 ± 0.0840	0.2182 ± 0.0730

A.3. Ablation Study

We conduct an ablation study to evaluate how hyperparameter choices affect our method’s accuracy. First, we vary the number of optimal images used for keyword extraction with gpt-4o from 5 to 10, 50, and 100 (Table A1, top) while fixing the number of extracted keywords at 5 (as in the primary analysis). Increasing the number of optimal images up to 50 leads to higher accuracy. This gain likely arises because relying only on top-ranked images may omit useful second- and third-ranked keywords; increasing the number of optimal images enables us to capture a broader range of selective keywords. However, after the number of optimal images reaches 100, the improvement ceases, likely because additional concepts cannot be adequately captured using only five keywords. These observations suggest that increasing the number of concepts could further improve accuracy.

Next, we compare accuracy when the number of extracted keywords from the optimal image set (using gpt-4o) is varied among 1, 5, and 10 (Table A1, middle) while fixing the number of optimal images at 50 as in the primary analysis. The results illustrate that increasing the number of output concepts from 1 to 5 boosts accuracy while pushing this number to 10 reduces accuracy. This decline may be caused by extracting irrelevant or noisy concepts. The improvement with five keywords suggests that voxels encode multiple concepts, but extracting too many can introduce noise. Increasing the number of optimal images, rather than keywords, might be a more effective method of capturing additional helpful concepts.

Finally, we compare three models for keyword extraction from the optimal image set: the large language model gpt-4o, an 8-bit quantized Llama3.1–70B (meta-llama/Llama-3.1–70B-Instruct), and the TextGraphParser (Li et al., 2023) used in MeaCap (Table A1, bottom). For gpt-4o and Llama3.1–70B-8bit, we use 50 optimal images and extracted five keywords, matching the primary analysis. For TextGraphParser, we use MeaCap’s default settings, extracting five image captions and up to four concepts per caption. Experimental results demonstrate that gpt-4o outperforms TextGraphParser, suggesting that an open-ended LLM-based approach to concept extraction is more effective than simply adopting words from captions, as TextGraphParser does. Moreover, comparing gpt-4o with Llama3.1–70B-8bit reveals that a higher-performance LLM can further boost accuracy. These findings imply that, as LLM capabilities continue to advance, so too does our framework’s potential to enhance the interpretability of voxel representations.

Prompt

The following are the result of captioning a group of images:

“Three people in a dark room with masks and lights.”

“A band is performing on stage with various instruments and lights.”

“A rock band is performing on a stage with a red Coca-Cola logo.”

“The image depicts a group of people singing together in a room.”

“A band is performing on stage with a singer holding a microphone and a guitarist playing his instrument.”

...

I am a machine learning researcher seeking to elucidate the concepts of this group in order to better understand my data.

Come up with 5 distinct concepts that are likely to be true for this group. Please write a list of captions separated by bullet points (“*”). For example:

* "a dog next to a horse"

* "a car in the rain"

* "low quality"

* "cars from a side view"

* "people in a intricate dress"

* "a joyful atmosphere"

Do not talk about the caption, e.g., "caption with one word" and do not list more than one concept. Also use singular form unless the concept naturally involves multiple objects.

The hypothesis should be a caption, so hypotheses like "more of ...", "presence of ...", "images with ..." are incorrect. Also do not enumerate possibilities within parentheses. Do not provide multiple options by using 'or' or '/' to maintain clarity. Here are examples of bad outputs and their corrections:

* INCORRECT: "various nature environment like lake, forest, and mountain" CORRECTED: "nature"

* INCORRECT: "a image caption of household object (e.g. bowl, vacuum, lamp)" CORRECTED: "a household object"

* INCORRECT: "Presence of baby animal" CORRECTED: "a baby animal"

* INCORRECT: "Different types of vehicles including cars, trucks, boats, and RVs" CORRECTED: "a vehicle"

* INCORRECT: "Image caption involving interaction between humans and animals" CORRECTED: "interaction between humans and animals"

* INCORRECT: "More realistic image" CORRECTED: "realistic image"

* INCORRECT: "Insect (cockroach, dragonfly, grasshopper)" CORRECTED: "a insect"

* INCORRECT: "newspaper or magazine" CORRECTED: "a print media"

Again, I want to identify the characteristics of this group. List properties that hold more often for the images in this group. Answer only with a list (separated by bullet points “*”). Your response:

Figure A2. The prompt used for summarizing the captions of optimal image groups with an LLM. The text in red represents the captions of the optimal image groups, which vary depending on the target voxel and the number of optimal images used. The blue number specifies the number of concepts, which was varied during the ablation study.

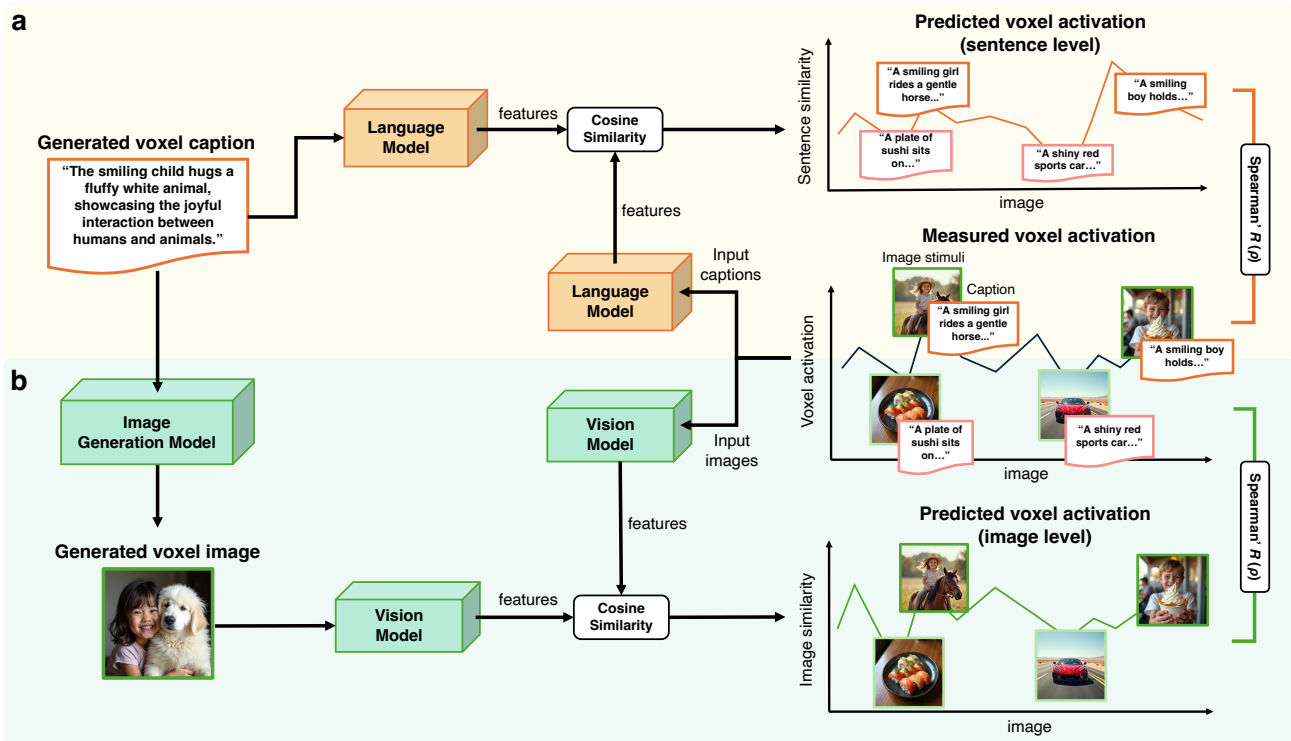


Figure A3. Overview of our evaluation methods. (a) We first obtain text embeddings for both the generated voxel captions (from the language model) and the NSD image captions. We then compute the cosine similarity between the voxel caption embeddings and each NSD caption embedding to derive a rough prediction of voxel activity. Finally, we evaluate text-level prediction performance by calculating Spearman’s rank correlation coefficient between these predicted values and the actual voxel responses. (b) We generate voxel images by visualizing voxel captions with an image generation model and, using the same vision model, compute vision-based embeddings for both the generated voxel images and the NSD image stimuli. As in (a), we compute the cosine similarity between voxel-image embeddings and NSD image embeddings and use Spearman’s rank correlation coefficient to evaluate image-level prediction performance.

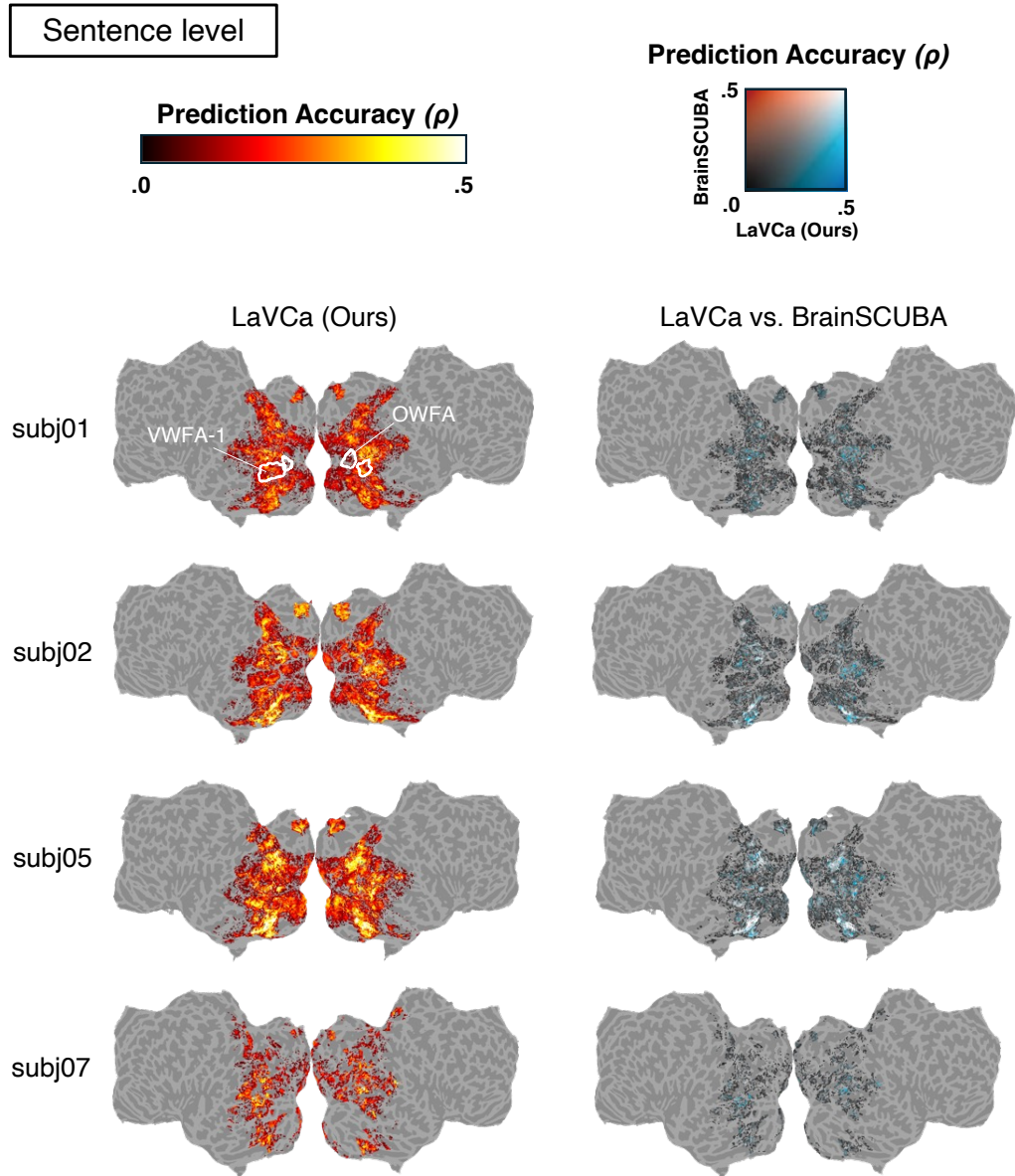


Figure A4. Mapping of brain activity prediction accuracy at the sentence level for LaVCa (left) and a comparison of brain activity prediction accuracy at the sentence level between LaVCa and BrainSCUBA (right) onto the flatmap for all subjects. The white outlines indicate Visual Word Form Area (VWFA-1) and Occipital Word Form Area (OWFA), which are ranked among the top two Words-category ROIs based on the mean number of voxels across subjects.

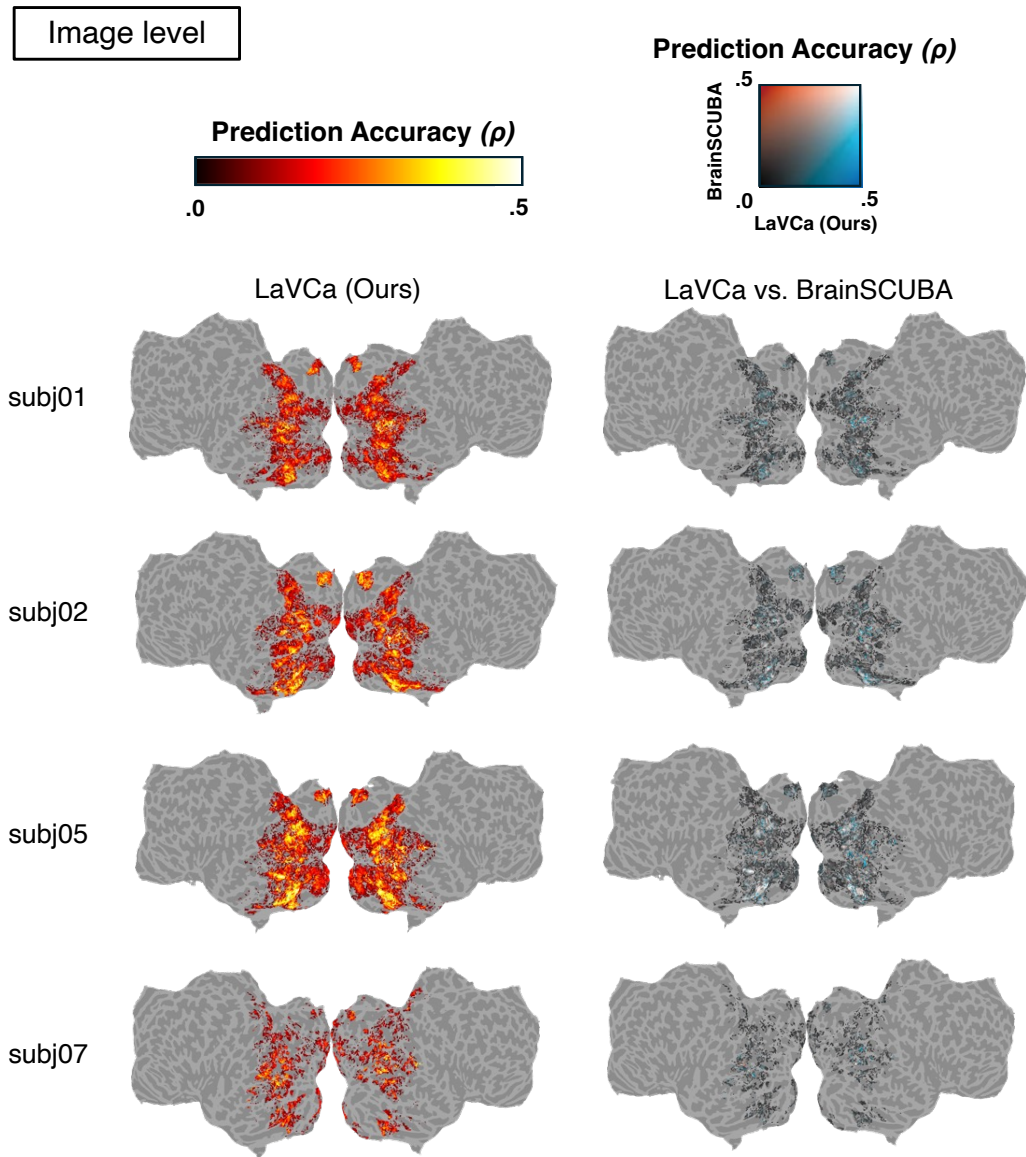


Figure A5. Mapping of brain activity prediction accuracy at the image level for LaVCa (left) and a comparison of brain activity prediction accuracy at the image level between LaVCa and BrainSCUBA (right) onto the flatmap for all subjects.

Table A2. Comparison of sentence-level brain activity prediction performance (all subjects). “Top-N voxels” refers to the voxels with top-N prediction performance in the training data. The results demonstrate the mean \pm standard deviation of prediction performance in the test data for each subject.

Top1000 voxels				
Model	subj01	subj02	subj05	subj07
Shuffled	-0.010 ± 0.281	0.094 ± 0.312	0.145 ± 0.331	0.013 ± 0.265
BrainSCUBA	0.291 ± 0.049	0.347 ± 0.062	0.378 ± 0.068	0.267 ± 0.055
LaVCa (Ours)	0.338 ± 0.051	0.392 ± 0.057	0.420 ± 0.061	0.320 ± 0.060
Top3000 voxels				
Model	subj01	subj02	subj05	subj07
Shuffled	0.000 ± 0.228	0.059 ± 0.255	0.099 ± 0.274	0.004 ± 0.205
BrainSCUBA	0.237 ± 0.057	0.284 ± 0.067	0.305 ± 0.077	0.212 ± 0.061
LaVCa (Ours)	0.280 ± 0.059	0.325 ± 0.068	0.349 ± 0.075	0.253 ± 0.069
Top5000 voxels				
Model	subj01	subj02	subj05	subj07
Shuffled	0.007 ± 0.199	0.058 ± 0.223	0.067 ± 0.243	0.009 ± 0.175
BrainSCUBA	0.207 ± 0.062	0.251 ± 0.071	0.264 ± 0.084	0.182 ± 0.065
LaVCa (Ours)	0.246 ± 0.066	0.287 ± 0.075	0.306 ± 0.084	0.218 ± 0.073
Top10000 voxels				
Model	subj01	subj02	subj05	subj07
Shuffled	0.008 ± 0.157	0.039 ± 0.178	0.051 ± 0.192	0.012 ± 0.134
BrainSCUBA	0.159 ± 0.071	0.195 ± 0.081	0.199 ± 0.095	0.134 ± 0.072
LaVCa (Ours)	0.191 ± 0.077	0.227 ± 0.086	0.237 ± 0.098	0.163 ± 0.081

Table A3. Comparison of image-level brain activity prediction performance (all subjects). "Top-N voxels" refers to the voxels with top-N prediction performance in the training data. The results show the mean \pm standard deviation of prediction performance in the test data for each subject.

Top1000 voxels				
Model	subj01	subj02	subj05	subj07
Shuffled	0.022 \pm 0.235	0.048 \pm 0.254	0.104 \pm 0.273	0.036 \pm 0.230
BrainSCUBA	0.278 \pm 0.056	0.322 \pm 0.052	0.357 \pm 0.057	0.262 \pm 0.061
LaVCa (Ours)	0.314 \pm 0.059	0.347 \pm 0.053	0.379 \pm 0.054	0.289 \pm 0.060
Top3000 voxels				
Model	subj01	subj02	subj05	subj07
Shuffled	0.017 \pm 0.187	0.059 \pm 0.210	0.087 \pm 0.228	0.007 \pm 0.174
BrainSCUBA	0.220 \pm 0.062	0.262 \pm 0.063	0.291 \pm 0.070	0.201 \pm 0.067
LaVCa (Ours)	0.248 \pm 0.066	0.286 \pm 0.063	0.315 \pm 0.068	0.221 \pm 0.069
Top5000 voxels				
Model	subj01	subj02	subj05	subj07
Shuffled	0.017 \pm 0.163	0.052 \pm 0.185	0.066 \pm 0.204	0.009 \pm 0.148
BrainSCUBA	0.188 \pm 0.067	0.226 \pm 0.070	0.250 \pm 0.078	0.169 \pm 0.069
LaVCa (Ours)	0.213 \pm 0.072	0.249 \pm 0.070	0.273 \pm 0.079	0.187 \pm 0.073
Top10000 voxels				
Model	subj01	subj02	subj05	subj07
Shuffled	0.010 \pm 0.128	0.034 \pm 0.145	0.049 \pm 0.159	0.006 \pm 0.114
BrainSCUBA	0.139 \pm 0.073	0.170 \pm 0.081	0.188 \pm 0.090	0.122 \pm 0.073
LaVCa (Ours)	0.160 \pm 0.078	0.191 \pm 0.082	0.208 \pm 0.092	0.138 \pm 0.077

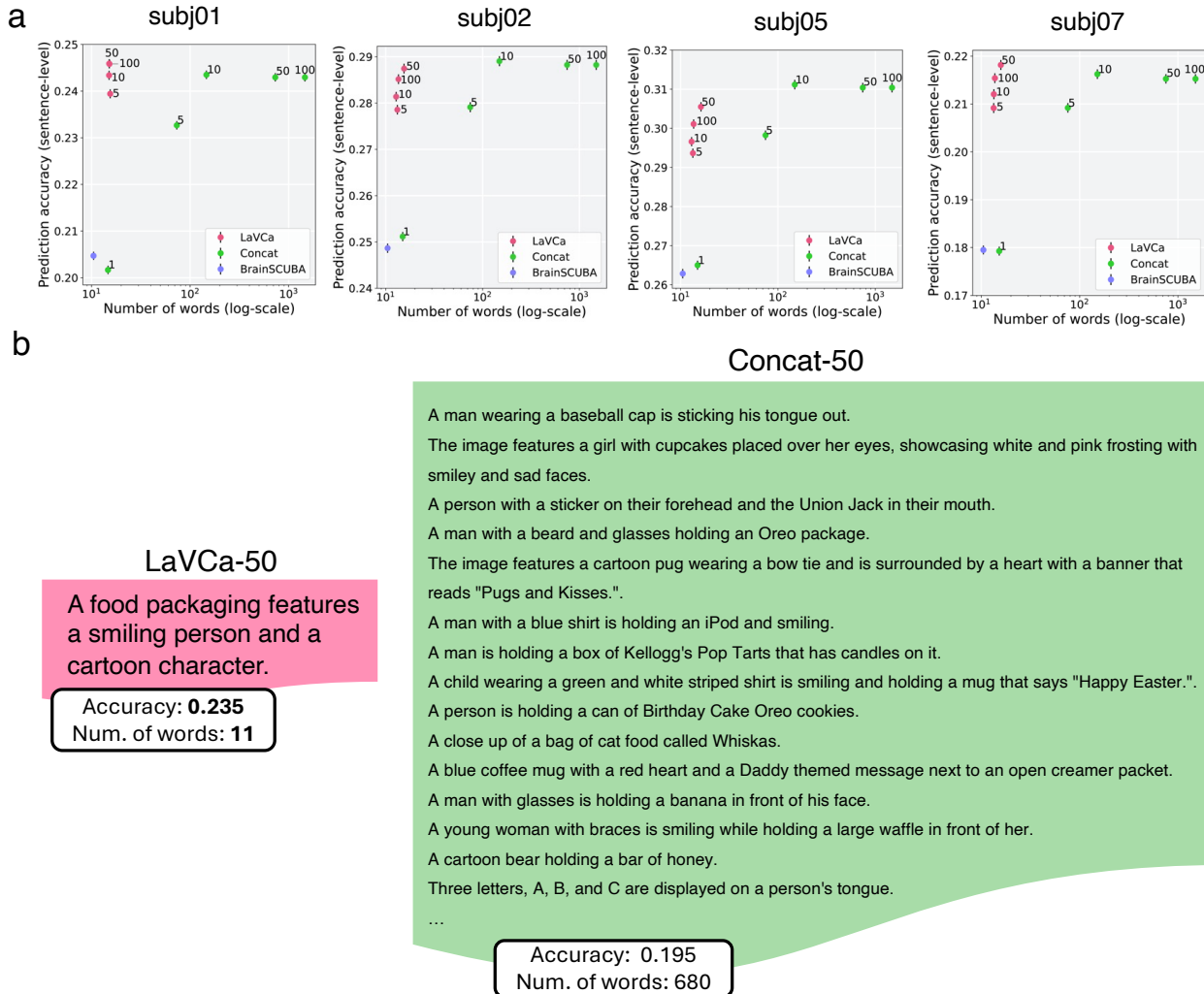


Figure A6. (a) Relationship between voxel caption prediction performance and word count (all subjects). The color of the plot corresponds to the lineage of each model. The numbers associated with LaVCa indicate the number of optimal images used for summarization, while the numbers associated with Concat represent the number of captions for concatenated optimal images. Error bars indicate the standard error. (b) Comparison of actual voxel captions between Concat-50 and LaVCa-50. Only a portion of the captions is depicted for Concat-50.

Table A4. Evaluation of the diversity of three models. PCs (90% Var) means the number of principal components required to explain 90% variance of the text embeddings. For intra-voxel comparisons, the mean \pm standard deviation across subjects is presented. The inter-subject average (Average) is presented as the mean \pm standard error.

Subject	Model	Acc.	Inter-voxel			Intra-voxel		
			Lexical	Semantic		Lexical		Semantic
			Vocab. size	Variance	PCs (90% Var)	Vocab. size	Length	Variance
subj01	BrainSCUBA	0.207 \pm 0.062	3400	0.0591	99	6.21 \pm 1.27	6.32 \pm 1.46	0.0163 \pm 0.0025
	Top-1 (Ours)	0.202 \pm 0.064	15384	0.0640	210	9.65 \pm 3.59	10.0 \pm 4.24	0.0194 \pm 0.0027
	LaVCa (Ours)	0.246 \pm 0.066	16477	0.0639	218	11.0 \pm 2.89	11.5 \pm 3.19	0.0198 \pm 0.0025
subj02	BrainSCUBA	0.251 \pm 0.071	3287	0.0591	133	6.17 \pm 1.32	6.27 \pm 1.51	0.0162 \pm 0.0026
	Top-1 (Ours)	0.251 \pm 0.070	14135	0.0632	206	9.99 \pm 3.65	10.5 \pm 4.28	0.0195 \pm 0.0027
	LaVCa (Ours)	0.287 \pm 0.075	17242	0.0639	218	11.3 \pm 3.64	11.8 \pm 3.93	0.0198 \pm 0.0027
subj05	BrainSCUBA	0.263 \pm 0.084	3043	0.0583	127	6.18 \pm 1.37	6.26 \pm 1.52	0.0159 \pm 0.0027
	Top-1 (Ours)	0.265 \pm 0.081	13485	0.0631	206	9.99 \pm 3.68	10.4 \pm 4.34	0.0195 \pm 0.0028
	LaVCa (Ours)	0.306 \pm 0.084	17459	0.0644	218	11.8 \pm 3.88	12.2 \pm 4.14	0.0199 \pm 0.0027
subj07	BrainSCUBA	0.182 \pm 0.065	3042	0.0587	131	6.23 \pm 1.30	6.36 \pm 1.47	0.0163 \pm 0.0026
	Top-1 (Ours)	0.179 \pm 0.066	12831	0.0632	203	10.1 \pm 3.51	10.6 \pm 4.14	0.0197 \pm 0.0026
	LaVCa (Ours)	0.218 \pm 0.073	16508	0.0646	222	11.6 \pm 3.76	12.0 \pm 4.02	0.0202 \pm 0.0026
Average	BrainSCUBA	0.226 \pm 0.019	3193 \pm 90	0.0588 \pm 0.0002	123 \pm 7.93	6.20 \pm 0.01	6.30 \pm 0.02	0.0162 \pm 0.0001
	Top-1 (Ours)	0.224 \pm 0.020	13959 \pm 545	0.0634 \pm 0.0002	206 \pm 1.44	9.93 \pm 0.10	10.4 \pm 0.132	0.0195 \pm 0.0001
	LaVCa (Ours)	0.264 \pm 0.020	16922 \pm 252	0.0642 \pm 0.0002	219 \pm 1.00	11.4 \pm 0.175	11.9 \pm 0.149	0.0199 \pm 0.0001

Table A5. The average prediction accuracy for each subject and the inter-subject average prediction accuracy when captions were shuffled within the ROI (Shuffled) and when they were used as-is (Original). For each subject, the average prediction accuracy \pm standard deviation is depicted, while for the inter-subject average, the average prediction accuracy \pm standard error is presented.

		Body areas		Face areas	
		EBA	FBA-2	OFA	FFA-1
subj01	Shuffled	0.035 \pm 0.147	0.014 \pm 0.128	0.031 \pm 0.067	0.017 \pm 0.113
	Original	0.169\pm0.105	0.124\pm0.102	0.083\pm0.069	0.117\pm0.083
subj02	Shuffled	0.010 \pm 0.144	0.026 \pm 0.109	0.036 \pm 0.071	0.024 \pm 0.097
	Original	0.158\pm0.101	0.128\pm0.103	0.079\pm0.066	0.105\pm0.078
subj05	Shuffled	-0.001 \pm 0.148	0.007 \pm 0.148	0.017 \pm 0.118	0.009 \pm 0.116
	Original	0.152\pm0.111	0.149\pm0.114	0.120\pm0.100	0.112\pm0.089
subj07	Shuffled	0.028 \pm 0.135	0.025 \pm 0.096	0.027 \pm 0.096	0.013 \pm 0.100
	Original	0.149\pm0.104	0.099\pm0.099	0.097\pm0.099	0.108\pm0.090
Average	Shuffled	0.018 \pm 0.008	0.018 \pm 0.005	0.028 \pm 0.004	0.016 \pm 0.003
	Original	0.157\pm0.005	0.125\pm0.010	0.095\pm0.009	0.111\pm0.003
		Place areas		Word areas	
		OPA	PPA	OWFA	VWFA-1
subj01	Shuffled	0.080 \pm 0.108	0.105 \pm 0.107	0.015 \pm 0.057	0.054 \pm 0.114
	Original	0.163\pm0.093	0.172\pm0.099	0.055\pm0.048	0.147\pm0.088
subj02	Shuffled	0.118 \pm 0.139	0.178 \pm 0.147	0.037 \pm 0.071	0.031 \pm 0.135
	Original	0.204\pm0.114	0.243\pm0.139	0.085\pm0.066	0.150\pm0.099
subj05	Shuffled	0.184 \pm 0.140	0.217 \pm 0.153	0.028 \pm 0.109	0.039 \pm 0.148
	Original	0.260\pm0.124	0.275\pm0.149	0.118\pm0.105	0.177\pm0.108
subj07	Shuffled	0.083 \pm 0.119	0.105 \pm 0.108	0.020 \pm 0.070	0.012 \pm 0.159
	Original	0.175\pm0.096	0.163\pm0.106	0.079\pm0.069	0.157\pm0.112
Average	Shuffled	0.116 \pm 0.024	0.151 \pm 0.028	0.025 \pm 0.005	0.034 \pm 0.009
	Original	0.200\pm0.022	0.213\pm0.027	0.084\pm0.013	0.158\pm0.007

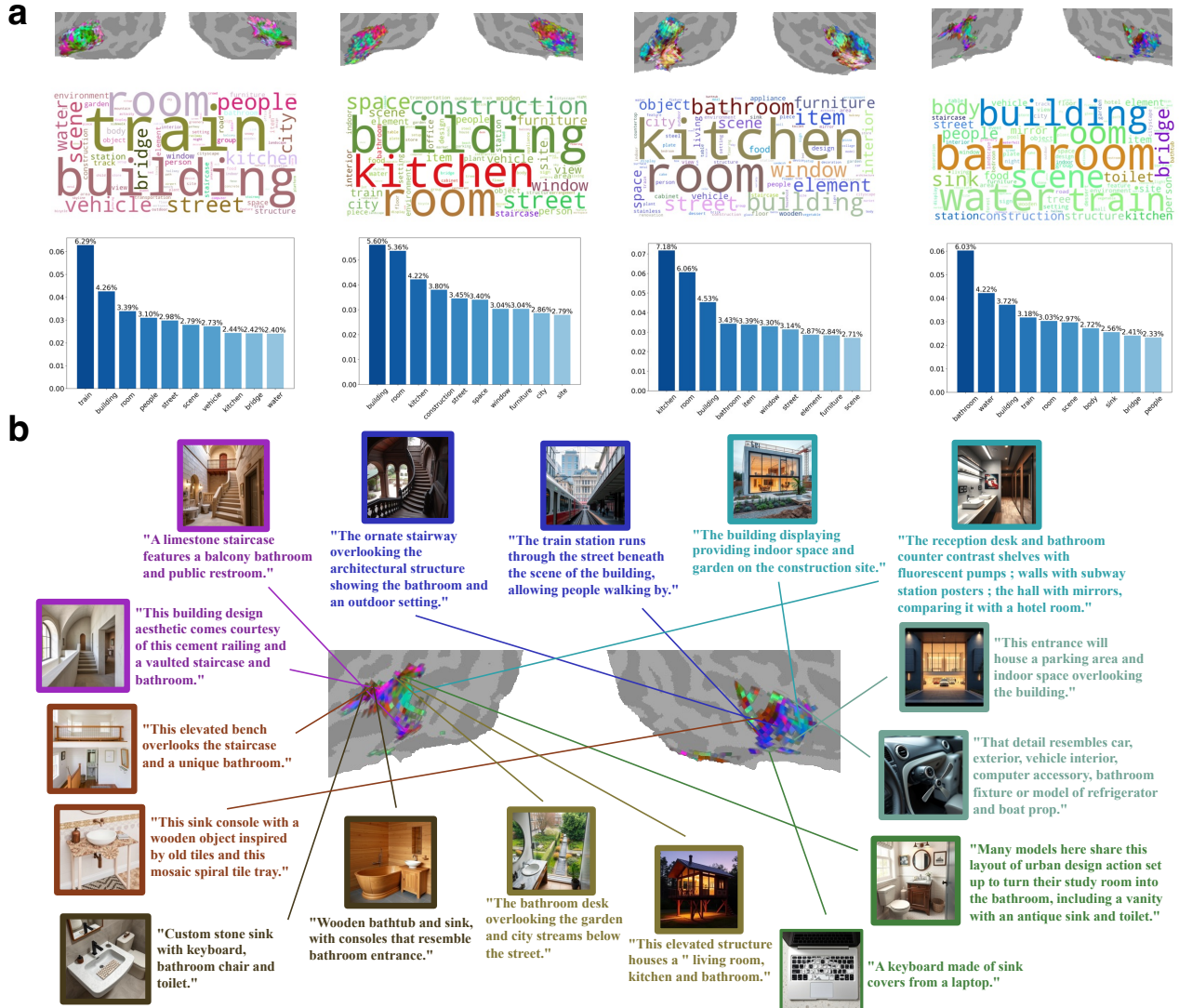


Figure A7. Interpretation of LaVCa captions in PPA. (a) The UMAP projection of text embeddings from captions onto the flatmap of all participants (top). A word cloud of the top 100 most frequent words (middle), with the colors in the word cloud corresponding to the flatmap. A bar graph of the top 10 most frequent words (bottom). (b) Visualization of the top 2 captions in terms of accuracy for eight clusters on the flatmap (subj07). The generated images corresponding to the captions are displayed to the left or above the captions. Voxels are connected to their corresponding captions and images with lines. The color of the captions and the frames of the generated images represents the average UMAP color of all voxels in the cluster.

LaVCa: LLM-assisted Visual Cortex Captioning

Examples of OFA (1/2)











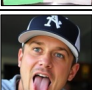

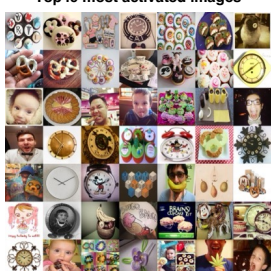
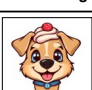


Voxel index: 270546		Model	Voxel caption	Voxel image	Acc. (Text-level)	Acc. (Image-level)	Vocab. size	Length	W2V variance
Top49 most activated images									
	LaVCa (Ours)	Each food item in the organizer and container bears a colored themed decoration with unique lettering or name brand logo.		0.1546	0.1034	14	14	0.02239	
	Top-1 (Ours)	Six different flavors of Pringles chips are lined up side by side.		0.06317	0.08339	8	9	0.02289	
	BrainSCUBA	A group of four hot dogs sitting on top of a table.		0.08565	0.05684	8	14	0.01494	
Voxel index: 296456		Model	Voxel caption	Voxel image	Acc. (Text-level)	Acc. (Image-level)	Vocab. size	Length	W2V variance
Top49 most activated images									
	LaVCa (Ours)	A child wearing a themed shirt, or someone else brandishing 50 smiling person holding a sign with the food network logo.		0.1229	0.03068	17	17	0.02000	
	Top-1 (Ours)	The storefront of PornTip Jewelry is brightly colored and has many items on display.		0.08345	0.02695	9	9	0.02171	
	BrainSCUBA	A store with a lot of signs on the wall.		0.06796	0.02664	5	5	0.01715	
Voxel index: 296535		Model	Voxel caption	Voxel image	Acc. (Text-level)	Acc. (Image-level)	Vocab. size	Length	W2V variance
Top49 most activated images									
	LaVCa (Ours)	A food packaging features a smiling person and a cartoon character.		0.2349	0.1999	8	8	0.01908	
	Top-1 (Ours)	A man wearing a baseball cap is sticking his tongue out.		0.1068	0.1146	7	7	0.01992	
	BrainSCUBA	A man with a toothbrush in his mouth.		0.09994	0.1482	4	4	0.01745	
Voxel index: 305512		Model	Voxel caption	Voxel image	Acc. (Text-level)	Acc. (Image-level)	Vocab. size	Length	W2V variance
Top49 most activated images									
	LaVCa (Ours)	Custom caricature logo illustration featuring the signature logo of puppy eyes complete with a clock face, child tooth and cute cupcake man.		0.1643	0.1186	18	19	0.02306	
	Top-1 (Ours)	The image shows a collection of cupcakes with various medical-themed decorations.		0.1239	0.1034	8	8	0.01930	
	BrainSCUBA	a close up of a tray of cupcakes on a bed		0.1084	0.1139	4	4	0.01847	

Figure A8. Comparison of voxel captions and voxel images in the OFA voxels of subj02 (1/2).

LaVCa: LLM-assisted Visual Cortex Captioning

Examples of OFA (2/2)



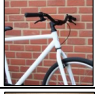













Voxel index: 305843		Model	Voxel caption	Voxel image	Acc. (Text-level)	Acc. (Image-level)	Vocab. size	Length	W2V variance
Top49 most activated images 		LaVCa (Ours)	Car boot handbag baked in good polka dot patterned bicycle dessert.		0.06425	0.1166	11	11	0.02518
		Top-1 (Ours)	A white bike with black handlebars is leaning against a red brick wall.		0.01513	0.08413	9	9	0.01963
		BrainSCUBA	A bicycle that is leaning against a wall.		0.008889	0.08090	8	14	0.01527
Voxel index: 296456		Model	Voxel caption	Voxel image	Acc. (Text-level)	Acc. (Image-level)	Vocab. size	Length	W2V variance
Top49 most activated images 		LaVCa (Ours)	The person holding an animal mouth is a person wearing glasses.		0.1225	0.07516	7	8	0.01924
		Top-1 (Ours)	A woman with a fake mustache and glasses.		0.04519	0.04770	5	5	0.02047
		BrainSCUBA	a close up of a person brushing her teeth		0.07279	0.03866	4	4	0.01651
Voxel index: 278988		Model	Voxel caption	Voxel image	Acc. (Text-level)	Acc. (Image-level)	Vocab. size	Length	W2V variance
Top49 most activated images 		LaVCa (Ours)	This is a fruit cake with banana icing and a decorative design.		0.06029	0.07104	7	7	0.01965
		Top-1 (Ours)	The image shows two bananas with faces drawn on them, placed on a blue and white striped cloth.		0.08880	0.1013	13	13	0.01781
		BrainSCUBA	A banana with a smiley face drawn on it.		0.1057	0.09654	5	5	0.01722
Voxel index: 305475		Model	Voxel caption	Voxel image	Acc. (Text-level)	Acc. (Image-level)	Vocab. size	Length	W2V variance
Top49 most activated images 		LaVCa (Ours)	Their food design and decoration scheme is paired with samples from holiday theme trucks.		0.1953	0.1583	10	10	0.02306
		Top-1 (Ours)	The image features a cowboy-themed birthday cake with number 3 on it, surrounded by cupcakes with hat toppers.		0.2178	0.1673	13	13	0.02264
		BrainSCUBA	A table topped with cakes and cup cakes.		0.2531	0.2058	5	6	0.01670

Figure A9. Comparison of voxel captions and voxel images in the OFA voxels of subj02 (2/2).

Examples of PPA (1/2)

Voxel index: 210730

Top49 most activated images		Model	Voxel caption	Voxel image	Acc. (Text-level)	Acc. (Image-level)	Vocab. size	Length	W2V variance
		LaVCa (Ours)	The digitally decorated room is a sign of the modern atmosphere.		0.2527	0.1728	7	7	0.02056
		Top-1 (Ours)	A restaurant called Fresco is next to another restaurant called Kabob.		0.1888	0.1307	7	9	0.01683
		BrainSCUBA	A view of a building with a lot of neon signs on it.		0.1576	0.0868	6	6	0.01636

Voxel index: 217592

Top49 most activated images		Model	Voxel caption	Voxel image	Acc. (Text-level)	Acc. (Image-level)	Vocab. size	Length	W2V variance
		LaVCa (Ours)	A shoe sole inside a cake depicting a chocolate mannequin.		0.2022	0.1828	8	8	0.02049
		Top-1 (Ours)	A pile of bread with a gold and black label on top.		0.1792	0.1155	7	7	0.01857
		BrainSCUBA	a close up of a stuffed animal on a bag		0.1340	0.1154	4	4	0.01653

Voxel index: 217647

Top49 most activated images		Model	Voxel caption	Voxel image	Acc. (Text-level)	Acc. (Image-level)	Vocab. size	Length	W2V variance
		LaVCa (Ours)	A bathroom fixture, newspaper slices and slices of some silver computer component, a wooden object, covered with the blue paint and pattern tool.		0.2786	0.2029	16	19	0.02198
		Top-1 (Ours)	The image showcases a pocket knife with various close-up views.		0.1775	0.1433	8	8	0.02239
		BrainSCUBA	a collage of photos with a green and black handle		0.2073	0.1223	5	5	0.01771

Voxel index: 217753

Top49 most activated images		Model	Voxel caption	Voxel image	Acc. (Text-level)	Acc. (Image-level)	Vocab. size	Length	W2V variance
		LaVCa (Ours)	This is the perfect urban setting, with a bridge deck and vehicle storage below.		0.1454	0.1109	9	9	0.01926
		Top-1 (Ours)	People are riding in small boats through a waterway at an amusement park with palm trees and a bridge in the background.		0.05586	0.03552	12	12	0.02358
		BrainSCUBA	a number of small boats in a body of water		0.06832	0.02745	5	5	0.01626

Figure A10. Comparison of voxel captions and voxel images in the PPA voxels of subj07 (1/2).

Examples of PPA (2/2)

Voxel index: 224691		Model	Voxel caption	Voxel image	Acc. (Text-level)	Acc. (Image-level)	Vocab. size	Length	W2V variance
	LaVCa (Ours)	A spiral staircase, an aerial view of the bathroom and a modern interior.		0.2733	0.2030	9	9	0.02184	
	Top-1 (Ours)	The image shows a bird's eye view of an artificial lake in the middle of a resort.		0.1005	0.1283	11	11	0.01993	
	BrainSCUBA	An aerial view of a large pool of water.		0.04142	0.1185	6	6	0.01630	
Voxel index: 239901		Model	Voxel caption	Voxel image	Acc. (Text-level)	Acc. (Image-level)	Vocab. size	Length	W2V variance
	LaVCa (Ours)	The pedestrian infrastructure shows a train station and railway track.		0.2759	0.4021	8	8	0.01811	
	Top-1 (Ours)	A railway track with a sign that says "Authorized personnel only."		0.1968	0.1826	9	9	0.02029	
	BrainSCUBA	A street sign on the side of a train track.		0.1597	0.2468	6	6	0.01369	
Voxel index: 239644		Model	Voxel caption	Voxel image	Acc. (Text-level)	Acc. (Image-level)	Vocab. size	Length	W2V variance
	LaVCa (Ours)	The wooden structure, with asian architecture, mirrors the zoo gate.		0.1727	0.09343	9	10	0.02312	
	Top-1 (Ours)	The image displays an outdoor Asian temple setting with various elements like a railing, steps, lanterns, and a roof.		0.1400	0.1539	15	17	0.02167	
	BrainSCUBA	A row of wooden benches sitting on top of a walkway.		0.1930	0.1348	7	7	0.01691	
Voxel index: 203319		Model	Voxel caption	Voxel image	Acc. (Text-level)	Acc. (Image-level)	Vocab. size	Length	W2V variance
	LaVCa (Ours)	The interior design highlighted a colorful nighttime scene and a water feature.		0.1364	0.1183	9	9	0.01651	
	Top-1 (Ours)	An ornate bathroom with green tiles, a wooden door, and stone wall.		0.2443	0.1894	10	11	0.01973	
	BrainSCUBA	A bathroom with a sink, mirror, toilet and bathtub.		0.2115	0.1972	7	8	0.01605	

Figure A11. Comparison of voxel captions and voxel images in the PPA voxels of subj07 (2/2).

OFA

LaVCa

BrainSCUBA

subj01



subj02



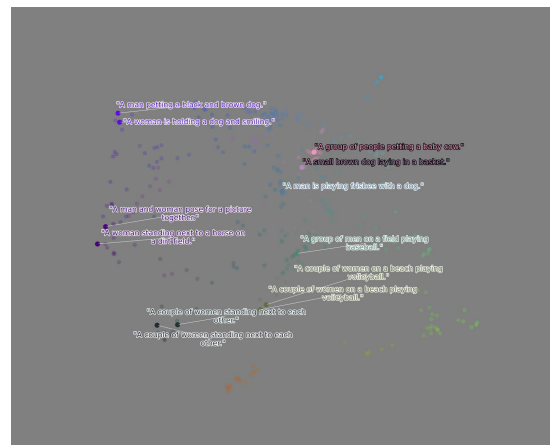
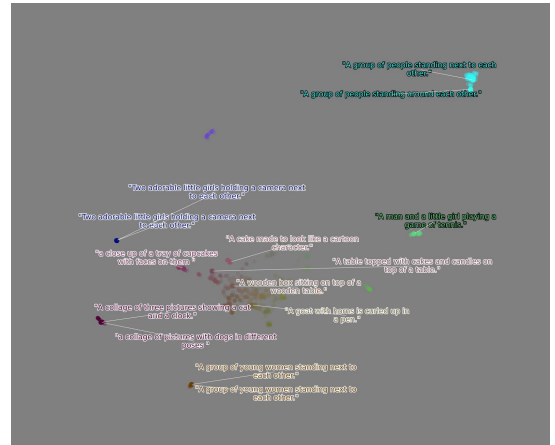
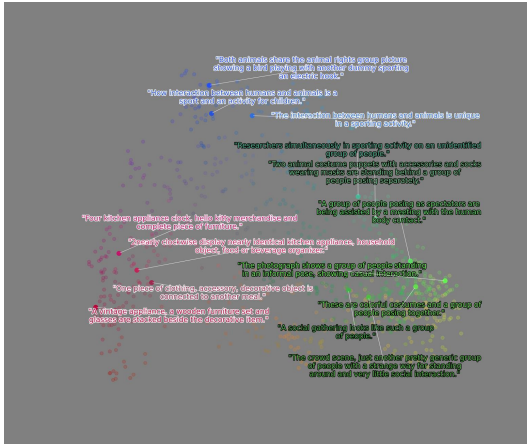
Figure A12. Visualization of OFA captions for subj01 and subj02. For each subject, the captions' UMAP representations were mapped onto a flatmap (top). The top 2 captions of each cluster in the UMAP space were visualized (bottom). The horizontal axis represents UMAP2, and the vertical axis represents UMAP1.

OFA

LaVcA

BrainSCUBA

subj05



subj07

Figure A13. Visualization of OFA captions for subj05 and subj07. The captions’ UMAP representations were mapped onto a flatmap (top) for each subject. The top 2 captions of each cluster in the UMAP space were visualized (bottom). The horizontal axis represents UMAP2, and the vertical axis represents UMAP1.

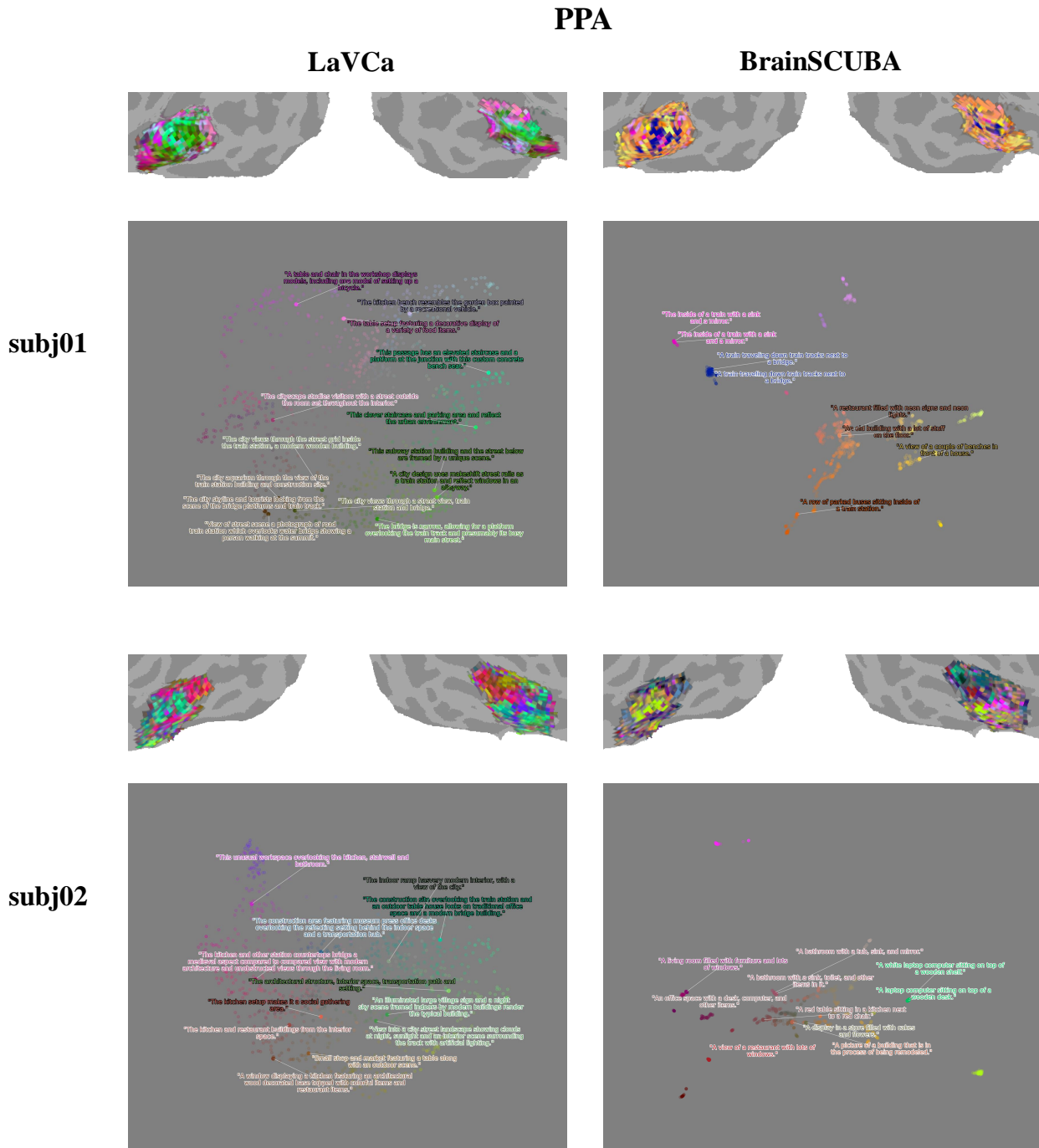


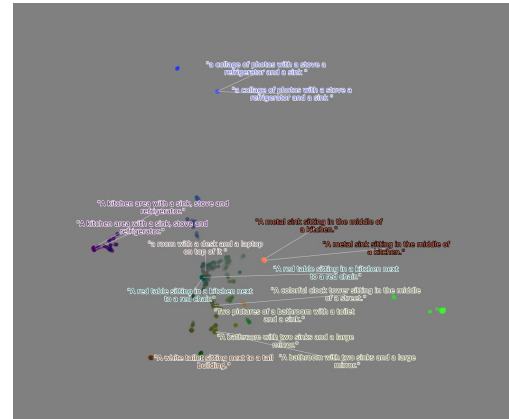
Figure A14. Visualization of PPA captions for subj01 and subj02. The captions' UMAP representations were mapped onto a flatmap (top) for each subject. The top 2 captions of each cluster in the UMAP space were visualized (bottom). The horizontal axis represents UMAP2, and the vertical axis represents UMAP1.

PPA

LaVCA

BrainSCUBA

subj05



subj07

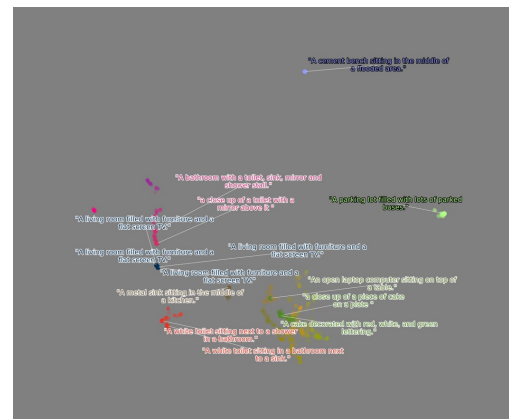
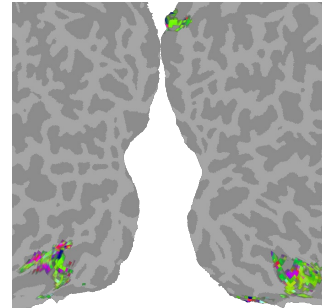
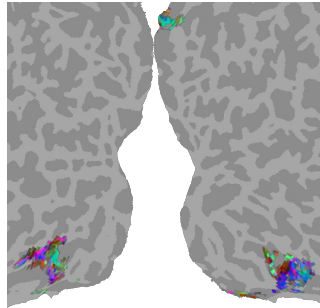


Figure A15. Visualization of PPA captions for subj05 and subj07. The captions' UMAP representations were mapped onto a flatmap (top) for each subject. The top 2 captions of each cluster in the UMAP space were visualized (bottom). The horizontal axis represents UMAP2, and the vertical axis represents UMAP1.